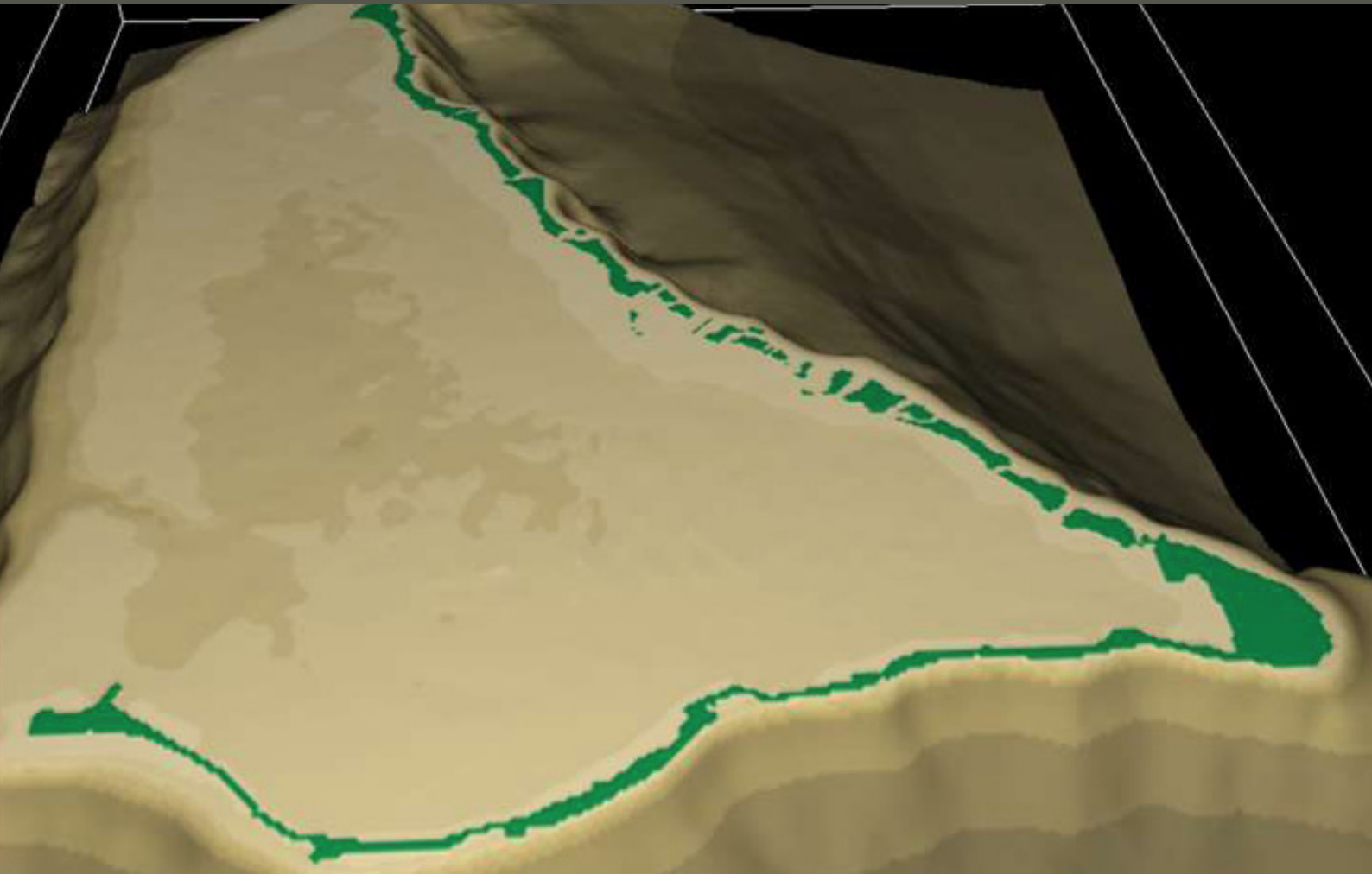# Bonriki Inundation Vulnerability Assessment

Development of severe and extreme scenarios of wave and water level through statistical analysis and numerical modelling Bonriki, Tarawa, Kiribati

Herve Damlamian, Cyprien Bosserelle, Jens Kruger,
Amrit Raj, Zulfikar Begg, Salesh Kumar, Aseri Baleilevuka

Bonriki Inundation Vulnerability Assessment (BIVA)

Development of severe and extreme scenarios
of wave and water level through
statistical analysis and numerical modelling
Bonriki, Tarawa, Kiribati

Herve Damlamian

Cyprien Bosserelle

Jens Kruger

Amrit Raj

Zulfikar Begg

Salesh Kumar

Aseri Baleilevuka

SPC
Secretariat
of the Pacific
Community

Table of Contents

List of Tables

List of Figures

Development of severe and extreme scenarios of wave and water level
through statistical analysis and numerical modelling
Bonriki, Tarawa, Kiribati

Acknowledgements

Development of severe and extreme scenarios of wave and water level
through statistical analysis and numerical modelling
Bonriki, Tarawa, Kiribati

List of Abbreviations

BIVA   Bonriki Inundation Vulnerability Assessment

CSIRO   Commonwealth Scientific and industrial Research Organisation

EVA   extreme value analysis

GDP   generalised Pareto distribution

GSD   Geoscience Division of Secretariat of the Pacific Community

Hs   significant wave height

HTGZ   Hawaii Tide Gauge Zero

IPCC   Intergovernmental Panel on Climate Change

MLOS   mean level of the sea

NCEP   National Centers for Environmental Prediction

NOAA   National Oceanic and Atmospheric Administration

PACCSAP   Pacific–Australia Climate Change Science and Adaptation Planning Program

POT   peaks-over-threshold

RCP   representative concentration pathway

Development of severe and extreme scenarios of wave and water level
through statistical analysis and numerical modelling
Bonriki, Tarawa, Kiribati

Executive Summary

Water levels in Betio (Tarawa, Kiribati) have been analysed to extract the tidal signal, the variability of the mean sea level and storm surge. The data were used to calculate the recurrence interval of extreme storm tide levels. It was found that the 100-year return event in Betio is 2.74 m above the tide gauge zero. The months with highest likelihood of flooding are March and October, mostly because the spring tides are larger during these months. However, this value does not include the contribution of waves to coastal flooding (i.e. wave set-up and infragravity waves).

A 100 m resolution wave model (open-source SWAN model) was developed based on downscaling of the 34-year hindcast wave model (Durrant et al. 2014). The model was calibrated against wave data collected during April–May 2013 on the reef slope off Bonriki. However, a satisfactory calibration could not be achieved in the lagoon under the easterly wave conditions of April–May 2013. During easterly wave conditions, waves refract around the atoll before entering the lagoon. This dissipates wave energy, resulting in small waves entering the lagoon. This study focuses on severe to extreme wave conditions. For the lagoon, high wave height is expected to be generated during westerly wave conditions. No westerly wave conditions were observed during April–May 2013.

The similar extreme wave distribution found by Ramsay et al. (2008) on the southeast corner of the lagoon, near Bonriki, provides confidence in the model's ability to simulate the westerly wave propagation into the lagoon.

In this study, the model outcome was used to investigate wave climate around Tarawa. Wave height time series were extracted on both side of Bonriki to enable extreme value analysis. The 100-year return interval wave heights were estimated as 1.0 m and 3.61 m in the lagoon and on the reef slope, respectively.

The extreme wave height distribution and the extreme storm tide level were combined into a joint probability of occurrence. Three scenarios were extracted from the 20-year, 50-year and 100-year return interval lines, generating nine scenarios of potential inundation events.

Finally, three climate change scenarios were used: RCP6 and RCP8.5 from the IPCC's AR5, and NOAA's intermediate–high scenario (Parris et al. 2012). For each climate change scenario, the sea level rise projection for 2064 was added to the storm tide level. A set of 36 scenarios were generated on each side of Bonriki, nine for the current sea level and nine for each of the three climate change scenarios.

The potential inundation under each scenario will be assessed in the BIVA inundation modelling report.

Development of severe and extreme scenarios of wave and water level
through statistical analysis and numerical modelling
Bonriki, Tarawa, Kiribati

1. Introduction

1.1. Background

The Bonriki Inundation Vulnerability Assessment (BIVA) project is part of the Australian government's Pacific–Australia Climate Change Science and Adaptation Planning Program (PACCSAP), within the International Climate Change Adaptation Initiative. The objectives of PACCSAP are to:

- improve scientific understanding of climate change in the Pacific;
- increase awareness of climate science, impacts and adaptation options; and
- improve adaptation planning to build resilience to climate change impacts.

The BIVA project was developed by the Geoscience Division (GSD) of the Secretariat of the Pacific Community (SPC) in partnership with the Australian government and the Government of Kiribati (GoK).

1.1.1. Project objective and outcomes

The BIVA project aims to improve our understanding of the vulnerability of the Bonriki freshwater reserve to coastal hazards and climate variability and change. Improving our knowledge of risks to this freshwater resource will enable better adaptation planning by the GoK.

More specifically, the project has sought to use this knowledge to support adaptation planning through the following outcomes:

- Improved understanding and ability to model the role of reef systems in the dissipation of ocean surface waves and the generation of longer-period motions that contribute to coastal hazards.
- Improved understanding of freshwater lens systems in atoll environments with respect to seawater overtopping and infiltration, as well as current and future abstraction demands, recharge scenarios and land-use activities.
- Enhanced data to inform a risk-based approach in the design, construction and protection of the Bonriki water reserve.
- Increased knowledge provided to the GoK and the community of the risks associated with the impact of coastal hazards on freshwater resources in response to climate change, variability and sea-level rise.

1.1.2. Context

The Republic of Kiribati is located in the Central Pacific and comprises 33 atolls in three principal island groups. The islands are scattered within an area of about 5 million square kilometres. The BIVA project focuses on the Kiribati National Water Reserve of Bonriki. Bonriki is located on Tarawa atoll within the Gilbert group of islands in Western Kiribati (Figure 1). South Tarawa is the main urban area in Kiribati, with the 2010 census recording 50,182 people of the more than 103,058 total population (KNSO and SPC 2012). Impacts to the Bonriki water resource from climate change, inundation, abstraction and other anthropogenic influences have potential for severe impacts on

Development of severe and extreme scenarios of wave and water level
through statistical analysis and numerical modelling
Bonriki, Tarawa, Kiribati

people's livelihood of South Tarawa. The Bonriki water reserve is used as the primary raw water supply for the Public Utilities Board (PUB) reticulated water system. PUB water is the source of potable water use by at least 67% of the more than 50,182 people of South Tarawa (KNSO and SPC 2012). Key infrastructure including the PUB Water Treatment Plant and Bonriki International Airport and residential houses are also located on Bonriki, above the freshwater lens, making it an important economic, social and cultural area for the Republic of Kiribati.
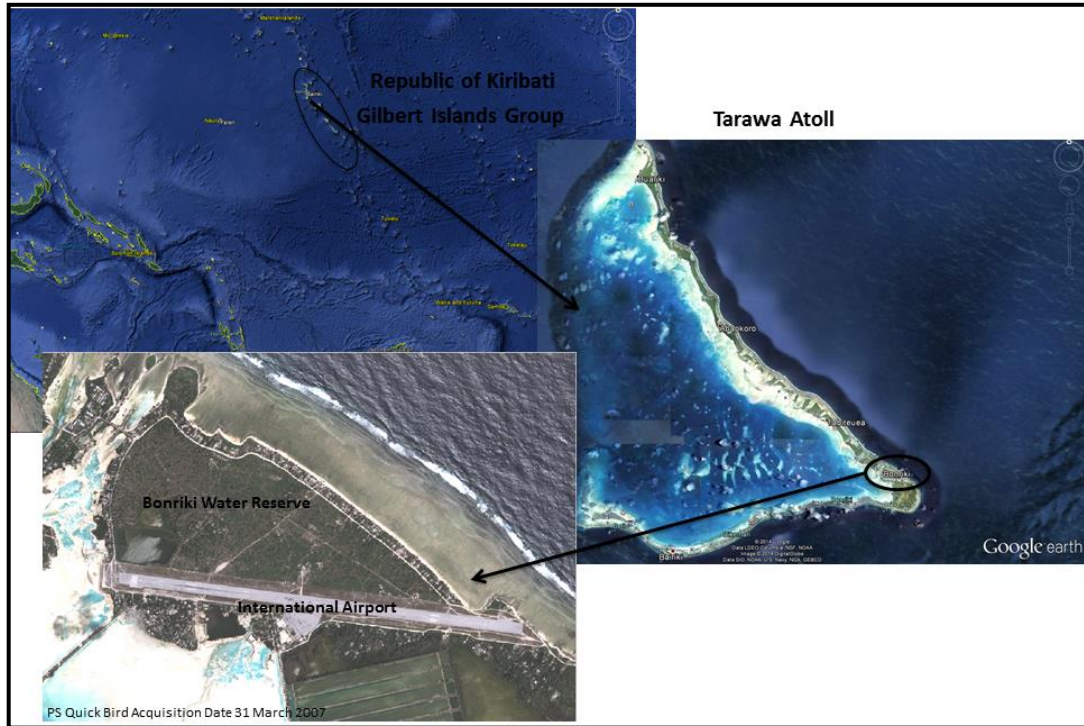
Figure 1. Bonriki Water Reserve Location.

1.2. Purpose of this report

This report provides details of the work undertaken as part of the BIVA project to develop probabilistic inundation scenarios to be fed into the inundation model for Bonriki. As illustrated in Figure 2, the project has three interlinked components: stakeholder engagement, groundwater investigation and analysis, and coastal investigation and analysis. The coastal investigation component of the project has been guided and supported by the stakeholder engagement component of the project. The outcome of the coastal work will be used as a baseline for the groundwater modelling activity.

Development of severe and extreme scenarios of wave and water level
through statistical analysis and numerical modelling
Bonriki, Tarawa, Kiribati
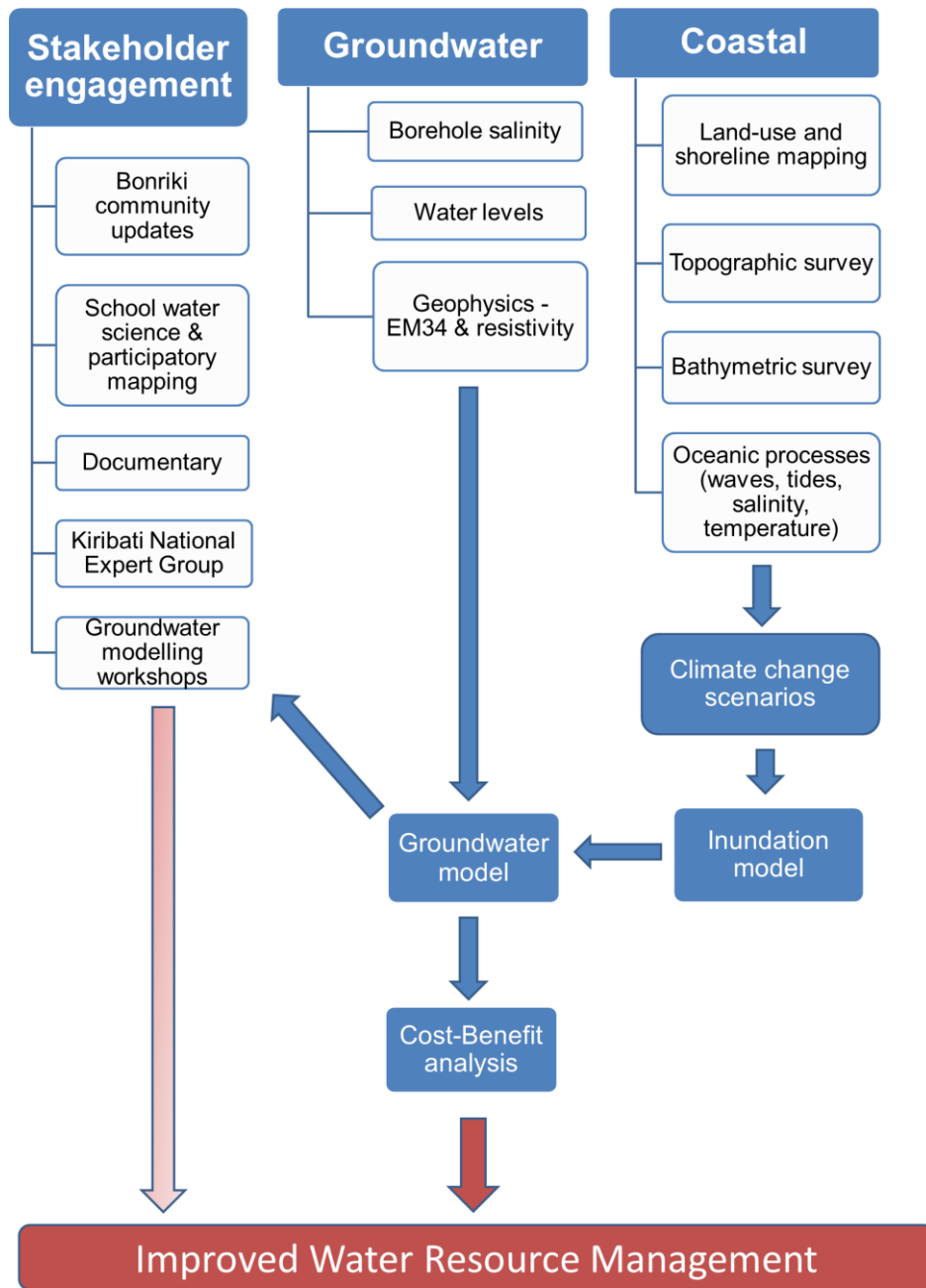
Figure 2. *Bonriki Inundation Vulnerability Assessment project components.*

1.3. Scope of this report

The coastal activities undertaken as part of the BIVA project will be fed into an inundation model – these activities include data collection on topography, bathymetry and oceanography, and development of the probabilistic inundation scenarios described in this report. These scenarios can be used to assess the inundation hazard at Bonriki.

- 'Overall methodology' describes the overall methodology and the approach taken for the study.
- 'Significant wave height' outlines the work undertaken to estimate the wave height distribution around Bonriki Islet.

Development of severe and extreme scenarios of wave and water level
through statistical analysis and numerical modelling
Bonriki, Tarawa, Kiribati

- 'Storm tide level' outlines the work undertaken to estimate the extreme distribution of storm tide around Bonriki Islet.
- 'Climate change projection' provides details on the climate change scenarios considered in this study.
- 'Joint probability of exceedance' provides the outcome of assessment of the joint probability of occurrence of high storm tides and large waves.
- 'Scenarios' gathers all the findings from the previous sections to develop 72 probabilistic scenarios.

2. Overall Methodology

The methodology used to develop inundation scenarios was adapted from Ramsay et al. (2008). Although Ramsay et al. (2008) provided a very comprehensive analysis of possible extreme wave and water level scenarios around south Tarawa, it did not include the Bonriki area, and the availability of a new dataset meant that this analysis needed to be revisited. The current study includes analysis of:

- a new bathymetry dataset around Bonriki (BIVA bathymetry report);
- a longer tidal record;
- new climate change scenarios (from the fifth assessment report of the Intergovernmental Panel on Climate Change); and
- a new 34-year wave hindcast model (Durrant et al. 2014) validated against wave buoys around the region; this model also provides full spectral wave information at unprecedented resolution for the Pacific region.

The methodology used to develop the scenarios is shown in Figure 3.

Extreme wave height distribution is based on the downscaling (100 m) of the PACCSAP wave hindcast model (Durrant et al. 2014), using the SWAN open-source wave model. This relatively high-resolution wave model benefits from new bathymetry data collected in the lagoon of Tarawa and around Bonriki Islet.

Extreme storm tide distribution on the ocean side and on the lagoon side of Bonriki is derived from more than 20 years of tide gauge data collected from the SEAFRAME gauge at Betio. The tide gauge is currently operated as part of the Australian-funded Climate and Oceans Support Program, COSPPac, in the Pacific.

The extreme distribution of wave and storm tide was then combined into a joint probability analysis. Based on the outcome of the joint probability and recent climate change projections (PACCSAP 2014), scenarios characterised by wave height, storm tide and climate change projections are developed.

Development of severe and extreme scenarios of wave and water level
through statistical analysis and numerical modelling
Bonriki, Tarawa, Kiribati
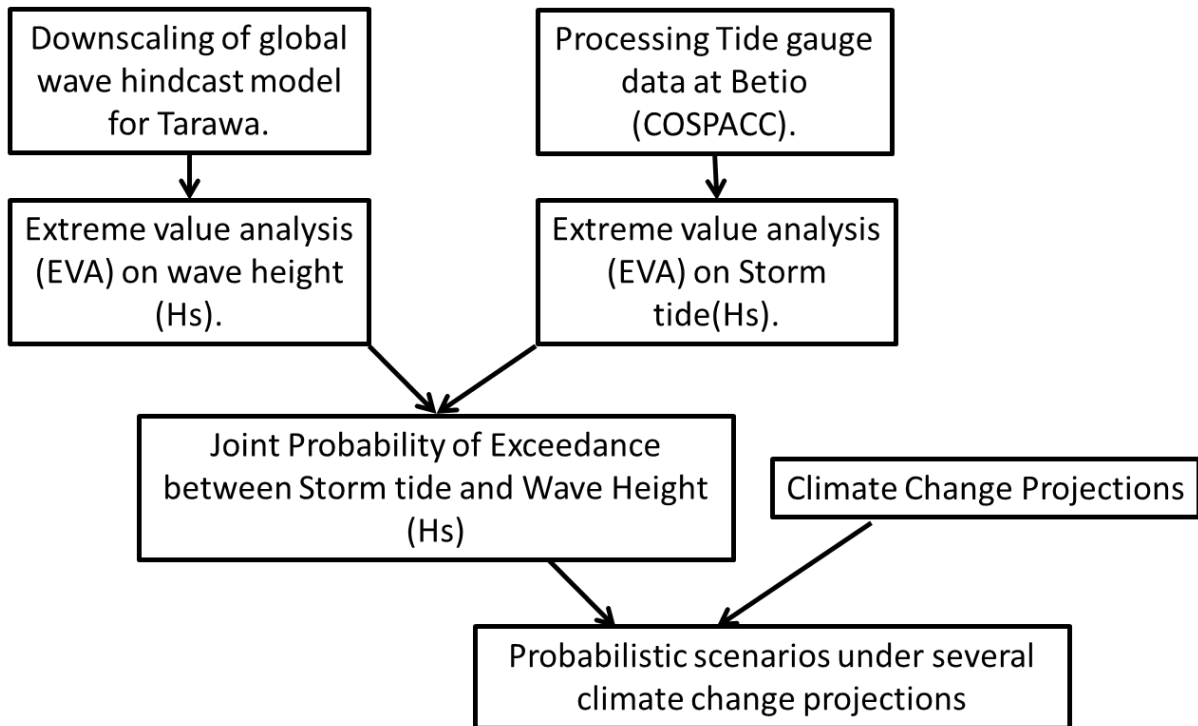
Figure 3. *Overall methodology.*

3. Significant Wave Height

3.1. Methodology

The recently completed Climate Forecast System Reanalysis by the National Centers for Environmental Prediction (NCEP) (Saha et al. 2010) provided higher-resolution wind hindcast. This gave the necessary baseline to build a higher wave hindcast model.

As part of the PACCSAP project, Durrant et al. (2014) generated a new, relatively high resolution wave hindcast model – the Wavewatch III (WW3) wave model (Tolman 1991, 2009) – that focused on the Pacific region. Figure 4 shows the resolution of the model output. The model was validated using wave buoys deployed at various locations around the Pacific by SOPAC and OCEANOR during the 1990s.

Development of severe and extreme scenarios of wave and water level
through statistical analysis and numerical modelling
Bonriki, Tarawa, Kiribati
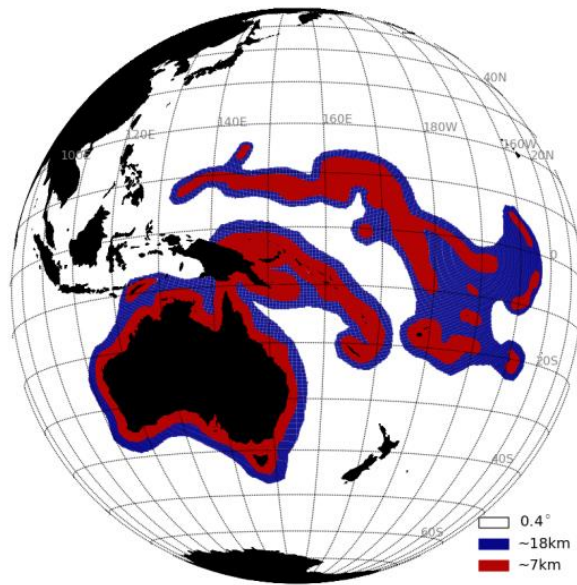
Figure 4. *Resolution of the WW3 wave model. Source: Durrant et al. (2014).*

This model was used to produce 34-year wave hindcast data (1979–2013), delivering spectral wave information at a resolution of 0.5 degrees, as well as wave parameters at a resolution of 4 minutes around the former SOPAC member countries. Under the current project, efforts were made to downscale the WW3 model and create a high-resolution wave hindcast dataset for Tarawa. A SWAN model with a resolution of 1 km was developed, covering Tarawa and its neighbouring islands.

A bathymetry grid (Figure 5), used as model input, was created using various sources of data:

- multibeam data from SOPAC collected under the 8th European Development Fund, EDF8, project around the rim of Tarawa atoll and in parts of the lagoon (shipping channel and various proposed aggregate resource areas);

- multibeam tracks off Tarawa from the National Oceanic and Atmospheric Administration (NOAA);

- single-beam data in Abaiang from SOPAC collected in 1999;

- satellite-derived bathymetry in Tarawa lagoon (SOPAC – EDF8 project); and

- data from the ETOPO2 global digital elevation model.

Development of severe and extreme scenarios of wave and water level
through statistical analysis and numerical modelling
Bonriki, Tarawa, Kiribati
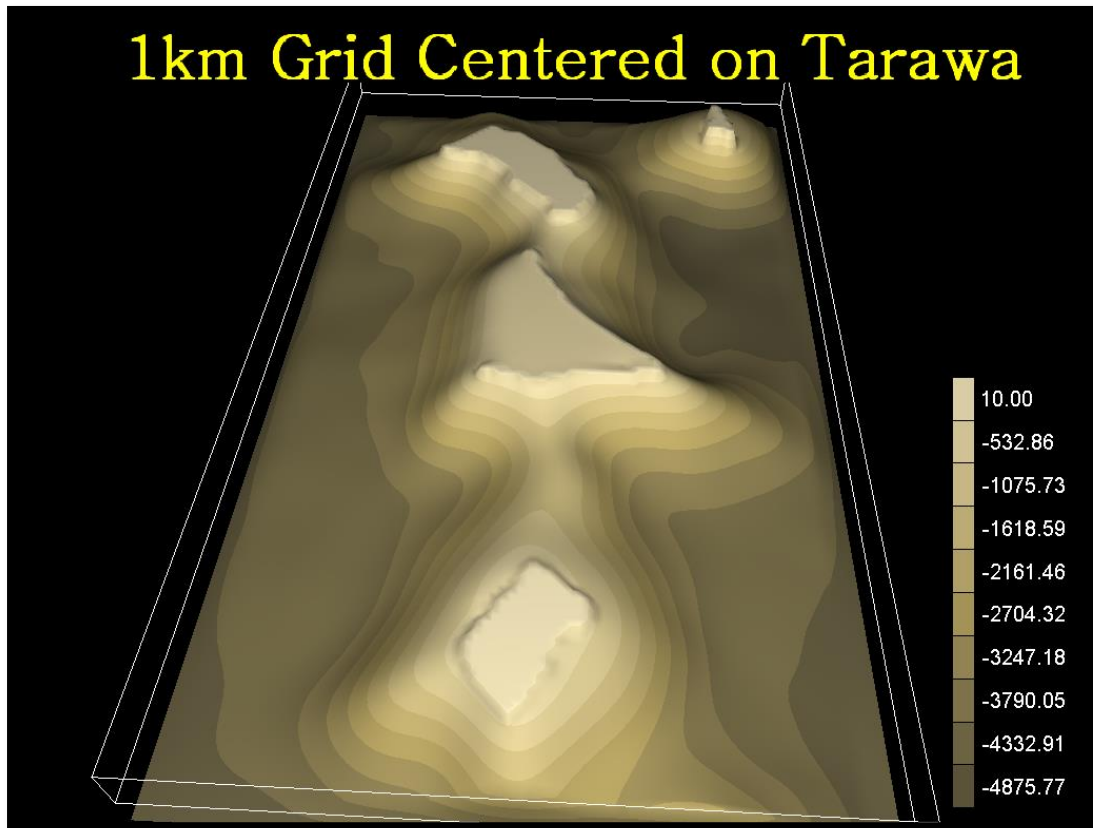
Figure 5. Three-dimensional view of the bathymetry of Tarawa and nearby islands from the 1km used in the SWAN model.

Directional wave spectral data from the WW3 model were extracted and fed into the 1-km-resolution SWAN model. Each of the four model boundaries is forced by three time series of directional wave spectra (hourly). Figure 6 shows model output locations, providing directional wave spectra information around Tarawa. Figure 7 shows an example of directional wave spectra information at a given location and a given time step.

The 1 km SWAN model is set up so that a local wind wave is generated from the Climate Forecast System Reanalysis wind data following a third-generation mode, with exponential growth and energy dissipation by white capping (as described by Komen et al. 1984). Finally, the model is also set up to account for nonlinear quadruplet wave interactions, depth-induced wave breaking and bottom friction (following Madsen et al. 1988).

Development of severe and extreme scenarios of wave and water level
through statistical analysis and numerical modelling
Bonriki, Tarawa, Kiribati
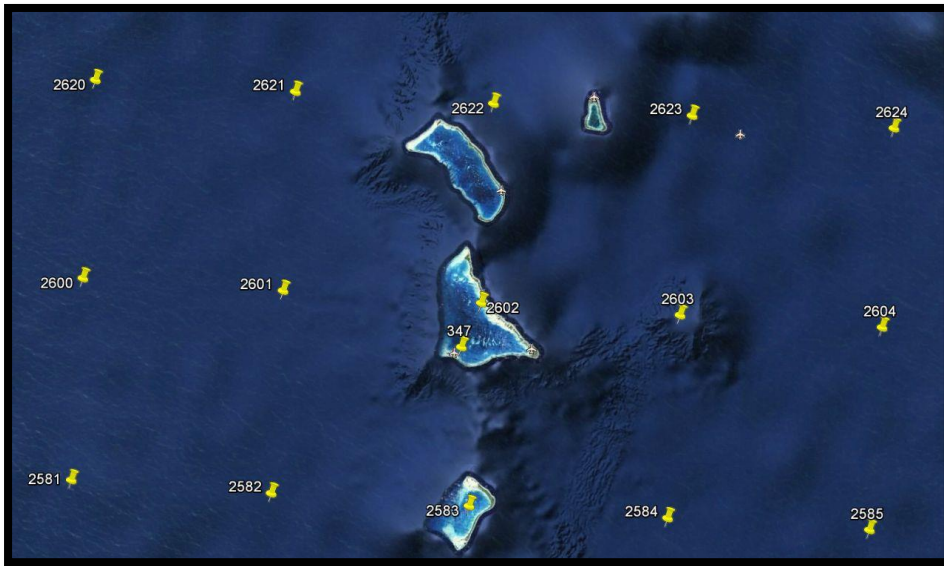
Figure 6. *Snapshot from Google Earth showing the locations around Tarawa to extract full wave spectrum data from the WW3 model.*
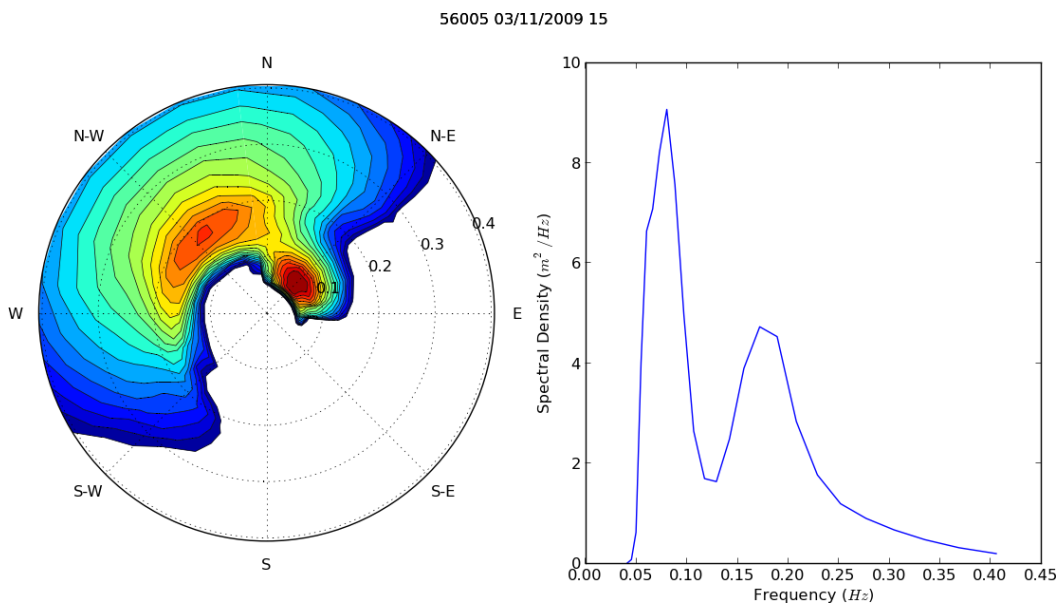
Figure 7. *Example of wave spectra extracted from the WW3 model. Source: Durrant et al. (2014).*

However, a model with 1 km resolution is too coarse to account for the type of small-scale features seen in Tarawa lagoon (e.g. shoals) or to appropriately represent the reef slope around the rim of the atoll. To scale the model down to an appropriate but manageable resolution, a 100 m–resolution model of Tarawa was nested into the 1 km–resolution SWAN model of Tarawa (Figure 8).

A bathymetry grid resolution of 100 m was developed using the data listed above, together with newly collected single-beam bathymetry data around Bonriki and along the western reef bordering Tarawa lagoon (BIVA bathymetry report). Finally, the Tanaea dredged channel near Bonriki was artificially closed so that waves on the lagoon side of Bonriki are either wind waves or swells that have entered the lagoon from the western side. The impact of easterly waves potentially

Development of severe and extreme scenarios of wave and water level
through statistical analysis and numerical modelling
Bonriki, Tarawa, Kiribati

propagating through the Tanaea channel to the lagoon side of Bonriki will be taken into account with the development of a high-resolution (10 m) inundation model (XBeach), which includes the generation and propagation of infragravity waves (BIVA inundation modelling report).
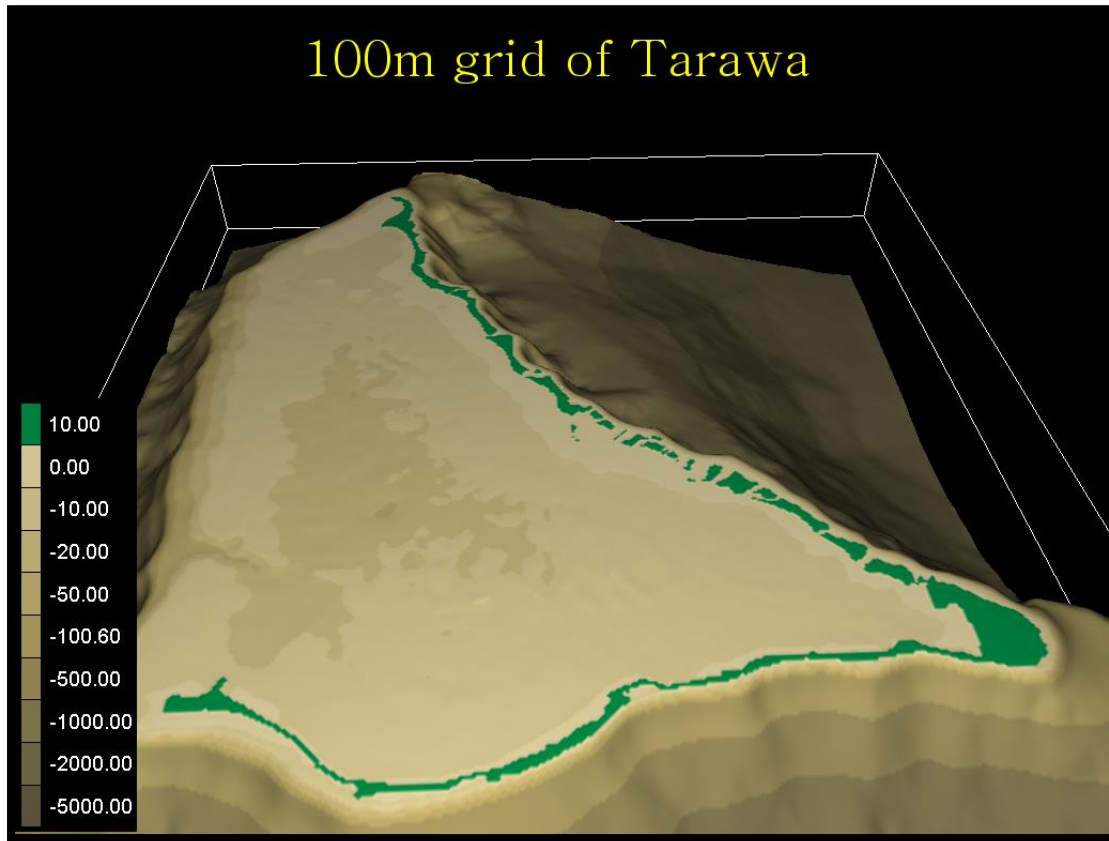
Figure 8. *Three-dimensional view of the bathymetry, with depth in meters, of Tarawa atoll from the 100 m grid used in SWAN.*

3.2. Model calibration

Oceanographic data were collected from April 2013 to April 2014 in Tarawa lagoon, and on the western and eastern reef slope. Details of data collection can be found in the BIVA oceanographic report.

As part of the PACCSAP project, Durrant et al. (2014) generated wave hindcast until May 2013. Thus, only oceanographic data collected before May 2013 can be used in the model calibration.

During April–May 2013, three instruments were deployed in Tarawa (Figure 9): two pressure sensors (TWR1 and TWR2) in the lagoon and another (TWR3) on the reef slope off Bonriki. The nested SWAN model was run for this two-month period, and the output of significant wave height (Hs) was compared with measured oceanographic data.

Development of severe and extreme scenarios of wave and water level
through statistical analysis and numerical modelling
Bonriki, Tarawa, Kiribati
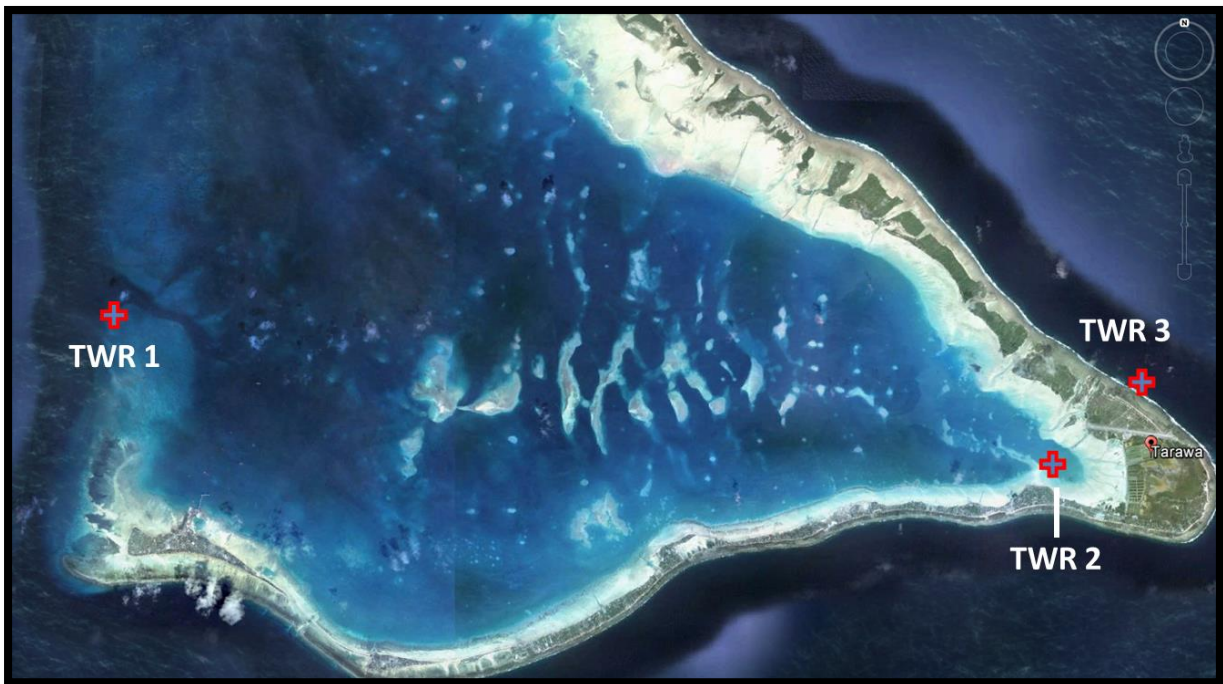
Figure 9. *Deployment locations for nearshore wave model calibration. Background is a satellite image of Tarawa lagoon.*

The good fit of the model was assessed through several skill scores.

- Root mean square error

$$RMSE = \sqrt{mean\left[(Hsc - Hsm)^2\right]}$$

where

Hsc is the computed significant wave height

Hsm is the measured significant wave height.

- Linear correlation coefficient

$$R2 = \frac{mean[(Hsc - mean[Hsc]) * (Hsm - mean[Hsm])]}{(std[Hsm] * std[Hsc])}$$

where

Hsc is the computed significant wave height

Hsm is the measured significant wave height

std is the standard deviation of the wave time series.

- Coefficient of variation of the root mean square error

$$SCI = \frac{RMSE}{mean[Hsm]}$$

Development of severe and extreme scenarios of wave and water level
through statistical analysis and numerical modelling
Bonriki, Tarawa, Kiribati

where

Hsc is the computed significant wave height

Hsm is the measured significant wave height

RMSE is the root mean square error.

- Relative bias

$$RELBIAS = \frac{mean[Hsc - Hsm]}{mean[Hsm]}$$

where

Hsc is the computed significant wave height

Hsm is the measured significant wave height.

- Brier skill score (Brier 1950).

The model shows good agreement with the wave data collected on the reef slope off Bonriki (Figure 10), with a linear correlation coefficient of 0.859 (

Development of severe and extreme scenarios of wave and water level
through statistical analysis and numerical modelling
Bonriki, Tarawa, Kiribati
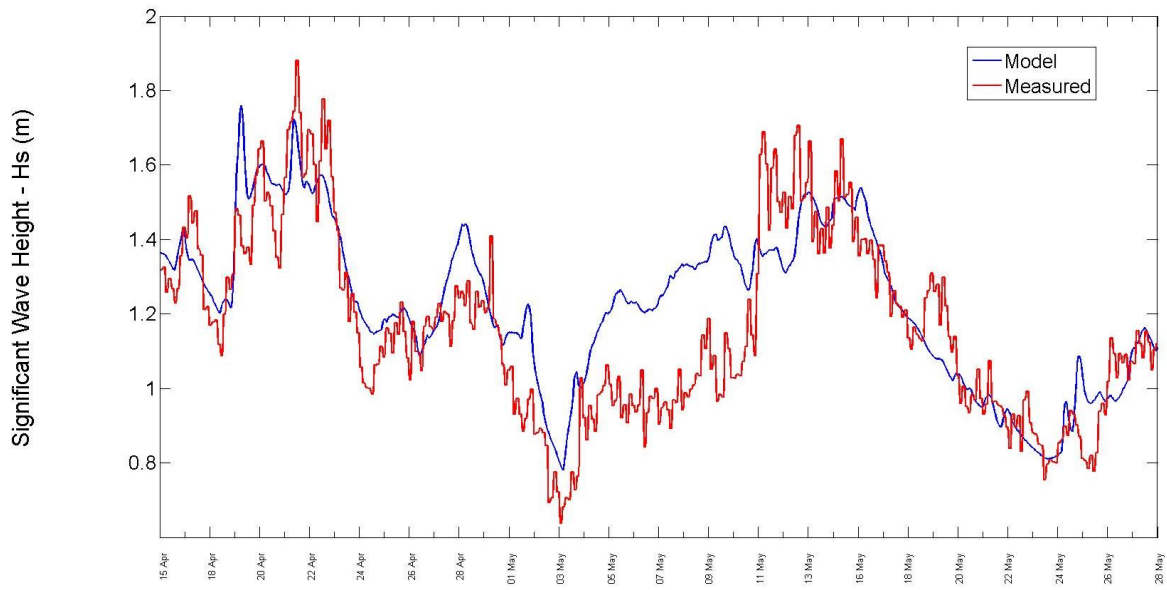
Table 1).

Figure 10. *Comparison between observed and simulated significant wave height on the reef slope off Bonriki (location of TWR3).*

Development of severe and extreme scenarios of wave and water level
through statistical analysis and numerical modelling
Bonriki, Tarawa, Kiribati

Table 1. Modelled wave height skill score on the reef slope off Bonriki.

	Linear correlation coefficient	Root mean square error	Coefficient of variation of root mean square error	Relative bias	Brier skill score
Eastern reef slope	0.859	0.160	0.134	0.0545	0.737

During April–May 2013, no westerly waves were recorded. Waves recorded in the lagoon originated from the refraction of the easterly offshore waves around the atoll. In the shipping channel (TWR1), the waves recorded are small, with a mean Hs of about 0.3 m. The model significantly overpredicts the wave height entering the lagoon, with a root mean square error of 0.21 m (Figure 11).

In the southeast corner of the lagoon near Bonriki (TWR2), both modelled and observed wave height were similar and almost zero (Hs < 5cm).
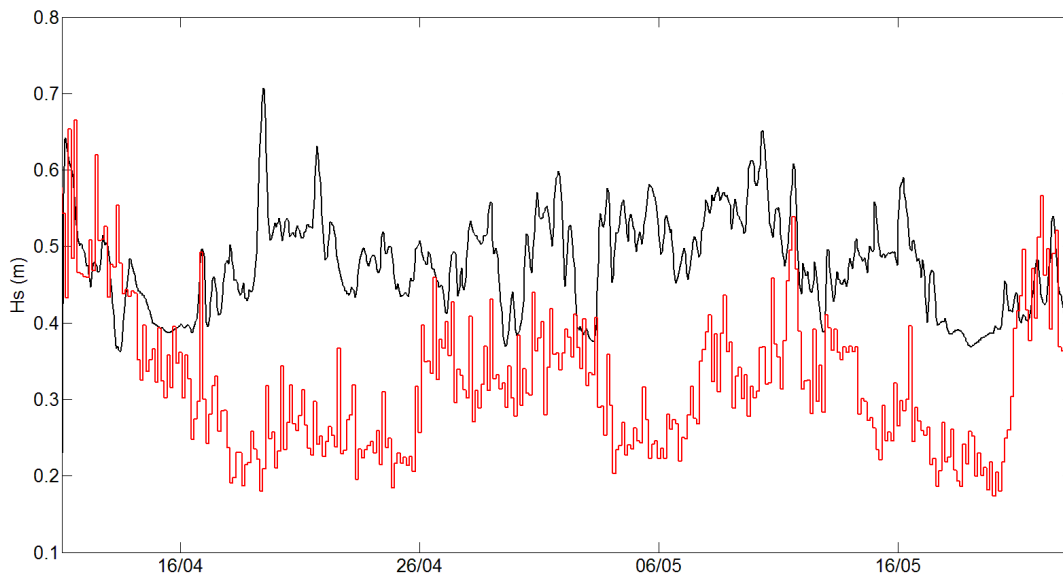
Hs = significant wave height

Figure 11. *Comparison between observed and simulated significant wave height near the shipping channel (TWR1) Red-observed; black-modelled.*

Although the model does not accurately simulate the refraction of the easterly waves entering the lagoon, these waves will most likely be ignored in this study. The wave data extracted from the model are used to perform extreme value analysis (EVA), so that only the greatest wave heights are considered. In the southeast corner of the lagoon, near Bonriki, the greatest wave heights are expected to be generated during westerly wave conditions.

The lack of westerly waves during April–May 2013 prevents a satisfactory calibration of the SWAN model in the lagoon. However, as seen below (under 'Results, Extreme conditions'), the results from the model for extreme distribution for lagoon waves are very similar to those of Ramsay et al. (2008).

Development of severe and extreme scenarios of wave and water level
through statistical analysis and numerical modelling
Bonriki, Tarawa, Kiribati

Once the spectral wave boundary is made available from the PACCSAP WW3 model (Durrant et al. 2014), a better assessment and calibration of the model can be performed using all observed data from April 2013 to April 2014, covering a broader range of directions for incident waves.

3.3. Results

3.3.1. Normal conditions

The nested SWAN model took several weeks to compute and generate 34 years of high-resolution hindcast wave data around Tarawa. The data were analysed to provide a better understanding of Tarawa's wind and wave climate.

In Tarawa, the trade winds control wind and wave climate (Figure 12, 13 and 14). Over the past 34 years, from January 1979 to May 2013, the wave climate has been dominated (96%) by easterly waves (30–150°).

The joint probability table between wave height and wave direction (Figure 14) also shows that waves around Tarawa are of relatively low height (Hs). Over the past 34 years, Tarawa experienced waves with an Hs lower than 2 m about 83% of the time, and waves higher than 3 m only 0.12% of the time.
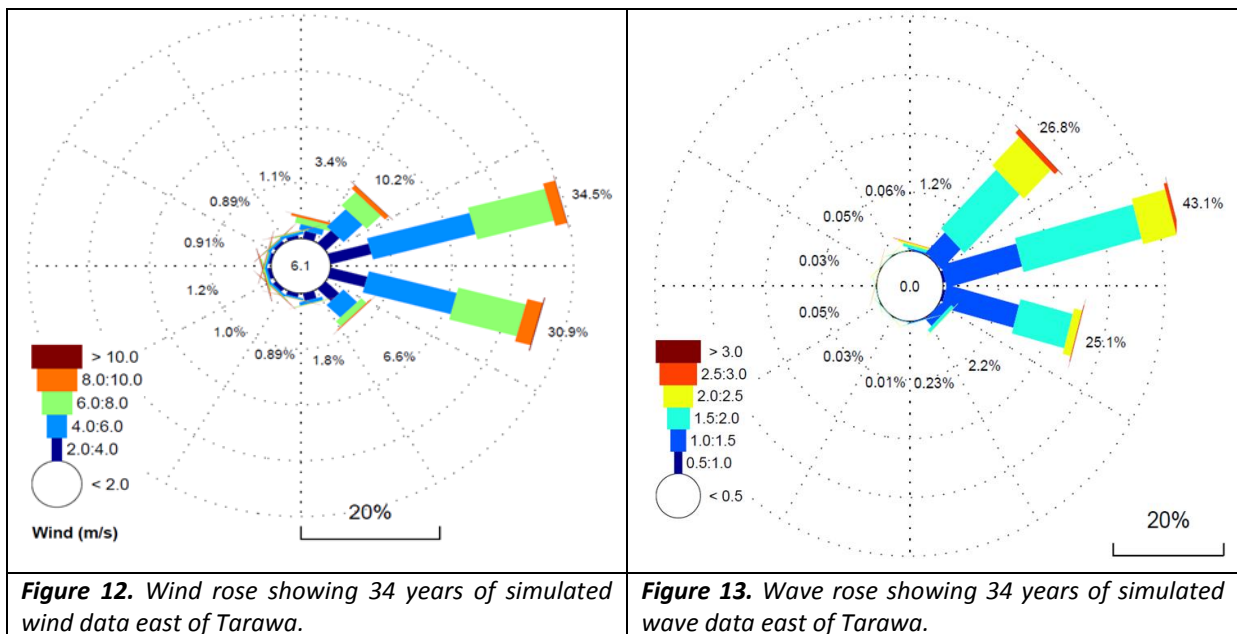
| **Figure 12.** Wind rose showing 34 years of simulated wind data east of Tarawa. | **Figure 13.** Wave rose showing 34 years of simulated wave data east of Tarawa. |

Development of severe and extreme scenarios of wave and water level
through statistical analysis and numerical modelling
Bonriki, Tarawa, Kiribati
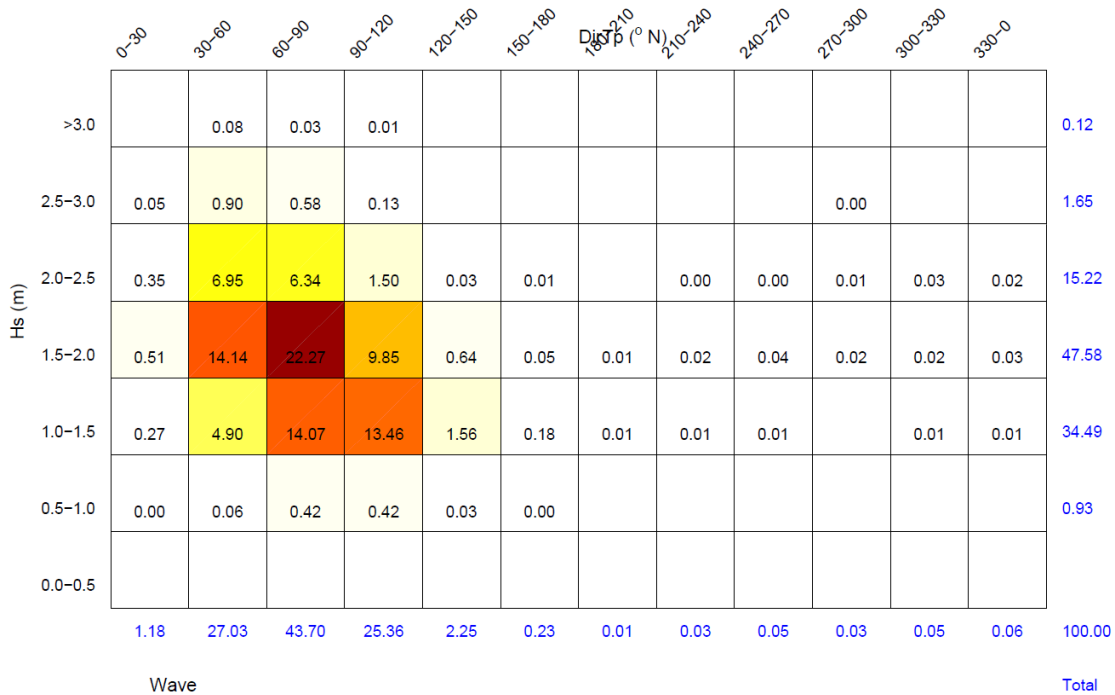
Hs = significant wave height

Figure 14. *Joint probability of wave height (rows) and wave direction (columns) calculated from the generated 34 years of wave hindcast off Bonriki (ocean side).*

3.3.2. Extreme conditions

Three EVA methods are commonly used:

- annual maxima method
- peaks-over-threshold (POT) method
- r-largest method.

For a 34-year record, the annual maxima method leads to a small data sample, which leads to large uncertainties in the results.

The POT method is generally believed to generate a better sample than the r-largest method (Coles 2001). All EVAs carried out in this study are based on the POT method. An example of use of the POT method on the deep-water Hs off Bonriki is shown in Figure 15.

Development of severe and extreme scenarios of wave and water level
through statistical analysis and numerical modelling
Bonriki, Tarawa, Kiribati
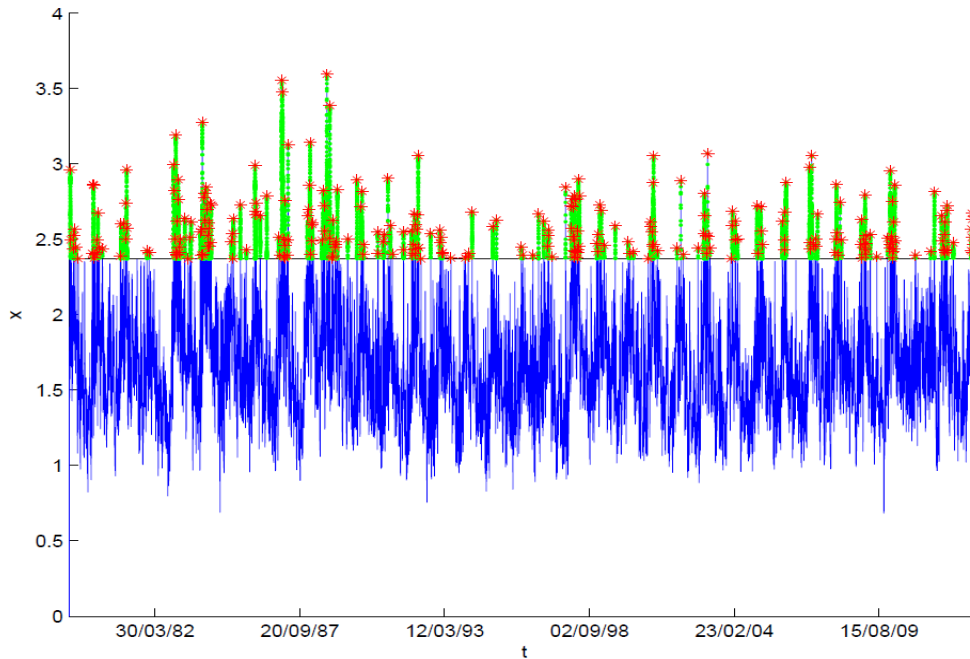
Figure 15. *Peaks-over-threshold analysis on the time series of significant wave height generated in deep water off Bonriki. The x axis has units of time with date labels, and the y axis is significant wave height in meters.*

The extreme wave height is investigated by performing an extreme distribution analysis, which consists of fitting the high historical wave height data onto a generalised Pareto distribution (GDP).

The wave height time-series data were extracted from the high-resolution wave model of Tarawa in two locations: on the lagoon (~5 m depth) and on the reef slope (~18 m depth) (Figure 16). For each dataset, the highest wave heights were selected by performing a POT analysis (Figure 15). Finally, each sample was fitted to a GDP (Figure 17 and 18).

The extreme distribution analysis quantifies the likelihood of an event as a probability of occurrence, given in this report as the annual return interval of the event. The EVA, threshold selection and confidence calculation were performed using the ORCA package (Deltares Systems 2012).

An Hs of 3.61 m has a 100-year return interval on the ocean side, whereas an Hs of 1.00 m has an estimated 100-year return interval on the lagoon side. This result is in close agreement with the work of Ramsay et al. (2008). Waves are generally small in the lagoon, because the dominant wave direction follows the easterly trade wind. When westerly waves enter the lagoon, Bonriki is still partially protected by the numerous shoals preventing wave propagation to the easternmost part of the lagoon.

Development of severe and extreme scenarios of wave and water level
through statistical analysis and numerical modelling
Bonriki, Tarawa, Kiribati

Figure 16. Extraction location for time series of wave height.
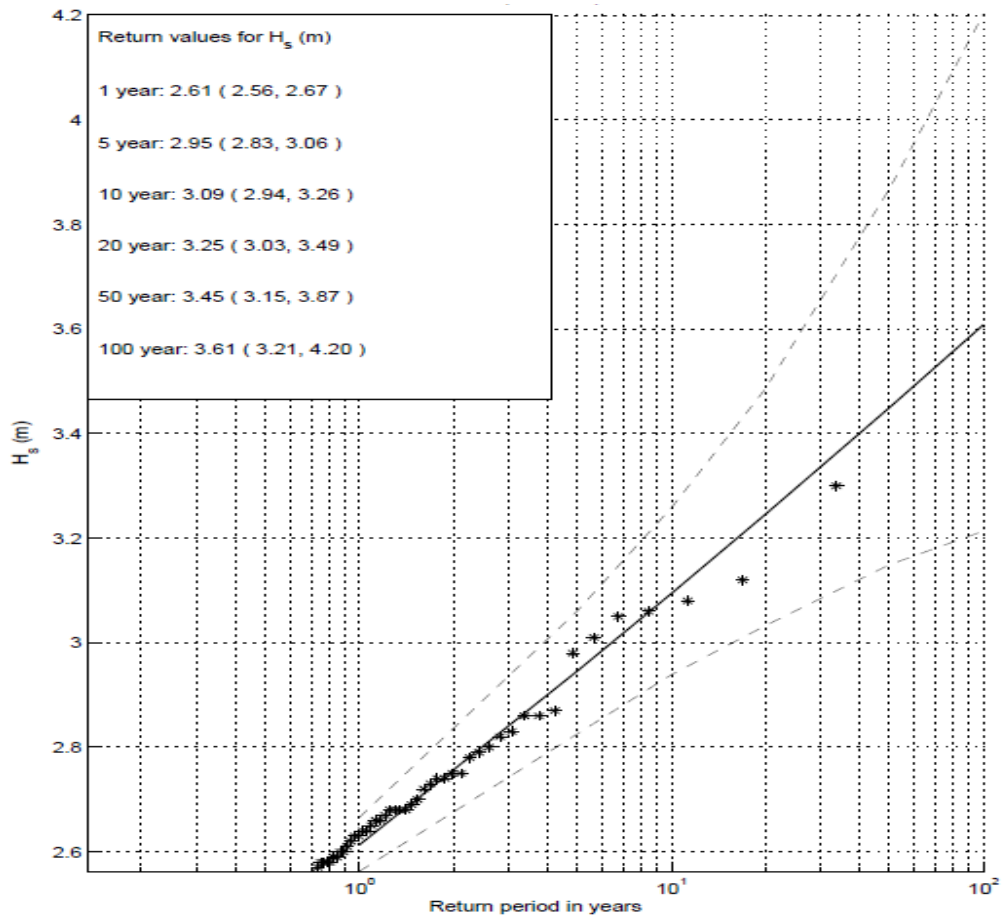
Hs = significant wave height

Figure 17. GDP fit and 95% confidence curve on the 34 years of wave data generated off Bonriki, on the reef slope (~18 m depth).

Development of severe and extreme scenarios of wave and water level
through statistical analysis and numerical modelling
Bonriki, Tarawa, Kiribati
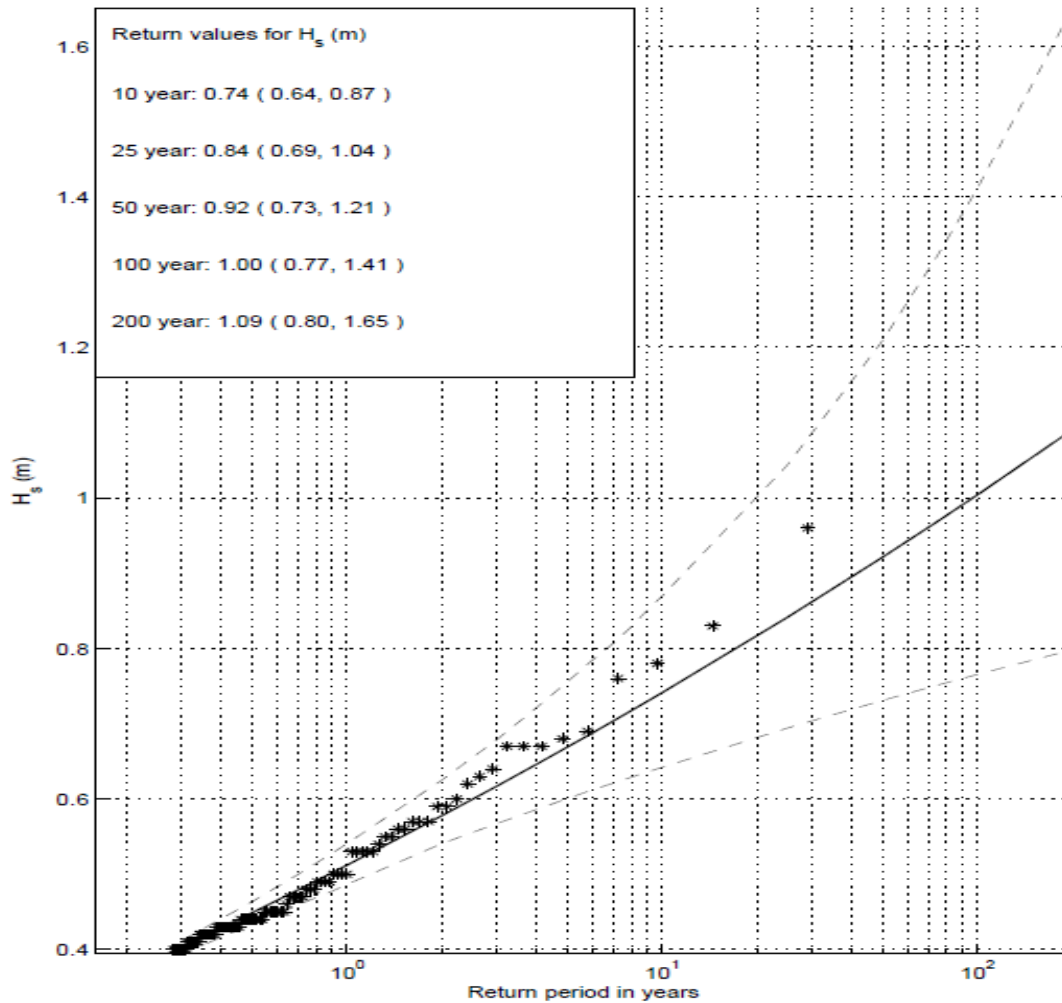
Hs = significant wave height

Figure 18. *GDP fit and 95% confidence curve on the 34 years of wave data generated off Bonriki, on the lagoon side (~5 m depth).*

3.4. Discussion

The outcome of the EVA offshore and on the lagoon side of Bonriki can be compared with the results found by National Institute of Water and Atmospheric Research (NIWA, New Zealand) under the Kiribati Adaptation Programme (Ramsay et al. 2008).

NIWA found a 100-year return interval for a deepwater Hs of 3.43 m east of Tarawa, based on the NOAA/NCEP Wavewatch hindcast for the period 1 February, 1997–1 November, 2007. Wave time-series data were extracted in deep water off Bonriki from our 1 km–resolution SWAN model of Tarawa. The EVA resulted in a 100-year return interval for an Hs of 3.74 m, with a 95% confidence interval of 3.41–4.26 m (Figure 19).

The significantly higher extreme wave condition for a 100-year return interval in this study is mainly due to the availability of a longer period of hindcast wave information. EVA is highly dependent on the length of the available dataset. The current study benefits from recent work under the PACCSAP project to develop a 34-year hindcast wave model. The 2008 study, based on a 10-year hindcast

Development of severe and extreme scenarios of wave and water level
through statistical analysis and numerical modelling
Bonriki, Tarawa, Kiribati

wave dataset from 1997, did not include peak wave height records of more than 3.5 m during the late 1980s (Figure 15), which significantly affect the outcome of the EVA.

Interestingly, the 100-year return interval Hs on the reef slope of Bonriki, at about 18 m depth, is 3.61 m. The lower extreme wave height can be attributed to energy dissipation due to wave refraction – that is, as a wave approaches the reef slope at an angle, the part of the wave crest closer to shore is in shallower water and moving more slowly than the part away from the shore, in deeper water. As the wave crest in deeper water catches up, the wave crest tends to become parallel to the reef crest.

Although the model shows good agreement with the observed wave data on the reef slope off Bonriki, a significant discrepancy was found between observed and computed wave height in the shipping channel, on the western reef slope. The model over-prediction could potentially be attributed to:

- error in the directional wave spectra information from the WW3 model;
- error associated with the model resolution, which does not appropriately resolve the complex bathymetry feature of the shipping channel; or
- error in modelling wave refraction around the atoll.

The EVA on the 34 years of wave hindcast data in the lagoon near Bonriki shows similar findings to the 2008 study. Ramsay et al. (2008) investigated possible extreme wave heights along the lagoon coastline of Tarawa. The two closest locations to the extraction point where we investigated extreme wave height distribution show Hs values for a 100-year return interval of 1.00 m and 1.11 m. This compares well with the outcome of this study (Hs= 1.00 m for a 100-year return interval), providing more confidence in the model performance for the lagoon.

Development of severe and extreme scenarios of wave and water level
through statistical analysis and numerical modelling
Bonriki, Tarawa, Kiribati
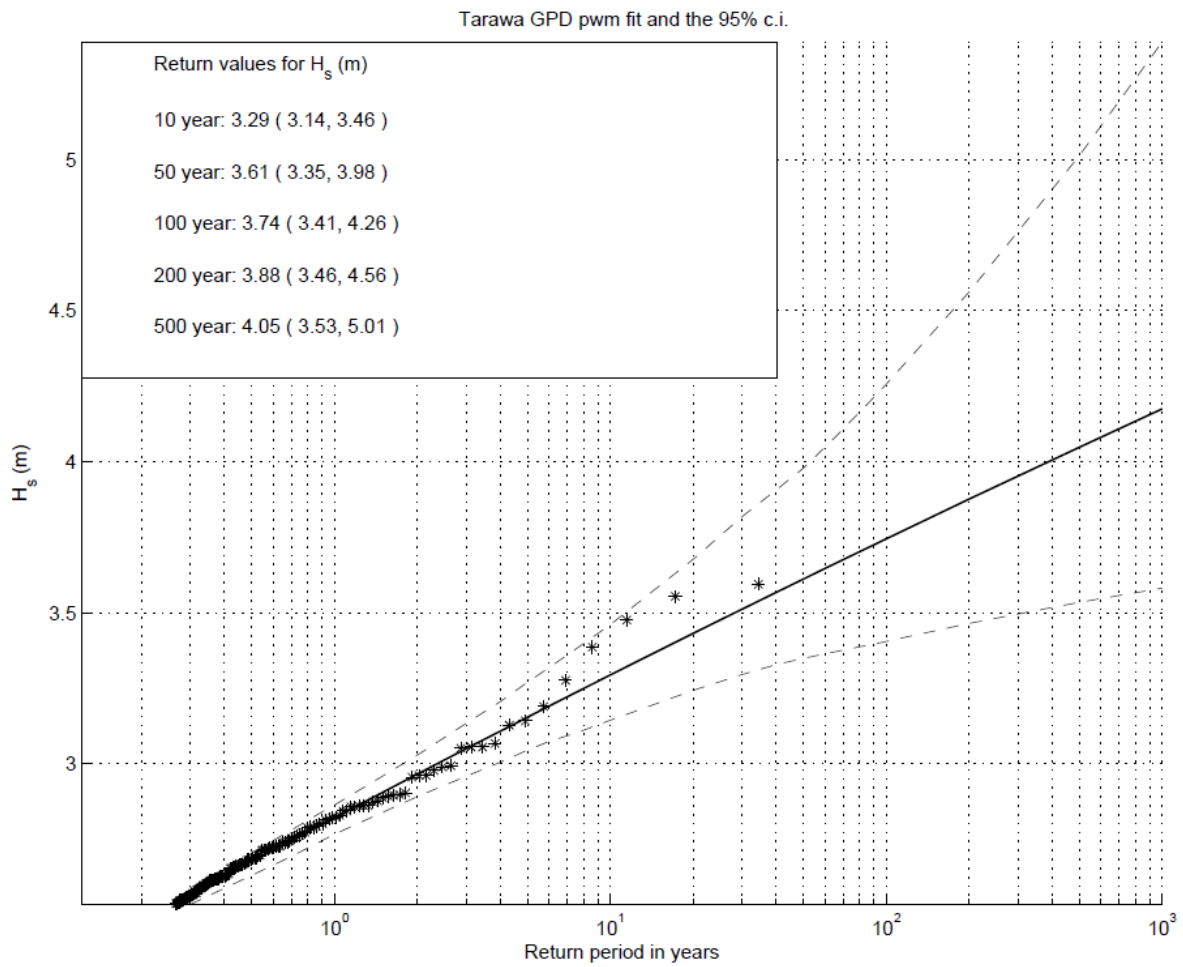
Hs = significant wave height

Figure 19. *GDP fit and 95% confidence curve on the 34 years of wave data generated off Bonriki in deep water.*

Development of severe and extreme scenarios of wave and water level
through statistical analysis and numerical modelling
Bonriki, Tarawa, Kiribati

4. Storm tide level

The western Pacific has been a focal point for research on mean sea level trends and variability in MLOS (e.g. Church et al. 2006; Merrifield et al. 2012; Meyssignac et al. 2012). In 2007, Tarawa was the focus of a comprehensive analysis of sea level, including an analysis of extreme water levels (Ramsay et al. 2008).

This study uses updated water levels recorded at Betio (on Tarawa atoll, Kiribati) between 1993 and 2014, to provide an updated analysis of extreme water levels and storm surges in Tarawa.

A comprehensive analysis of the water level at Betio has been compiled by Ramsay et al. (2008), who used a water level reconstruction based on deployment of three tide gauges in Tarawa to obtain a time series long enough (32.7 years) to analyse extreme water levels. The report gives a detailed analysis of the tide, the extreme water levels, storm surge, wind set-up and wave set-up. Ramsay et al. (2008) found that the MLOS trend in Tarawa was 2.7 mm/year, using the duration of the sea level reconstruction. They also presented an analysis of the monthly MLOS and found a correlation between the MLOS and the Southern Oscillation Index. The analysis by Ramsay et al. (2008) was carefully done; the current report extends the analysis using the most recent data on water levels.

4.1. Methodology

This study uses the water level recorded at the SEAFRAME gauge, installed at Betio in December 1992 by the Australian Bureau of Meteorology (BoM 2010). The data provide a 21-year record based on a single location. No reconstruction has been used to extend the dataset, to avoid introducing potential errors from previous tide gauges.

The dataset provided by the Australian Bureau of Meteorology (under the Climate and Oceans Support Program in the Pacific) contains the water level relative to the SEAFRAME gauge benchmark, the tidal residual (i.e. the deviation from the predicted tide) and the tidal residual corrected for the effect of atmospheric pressure.

The tide was analysed using the tidal harmonic analysis software T_TIDE (Pawlowicz et al. 2002). The exceedance curve was generated by analysing high tides and statistically sampling the hourly tidal signal to generate a 100-year dataset used to calculate percentiles of exceedance of high tides.

The tidal residual was obtained by subtracting the predicted tide from the raw water level. The tidal residual was then detrended and decomposed into signals of various periods. This process used a wavelet filter applied on different time windows (Figure 23).

The MLOS was calculated by using a wavelet low-pass filter with period longer than 32 days. The MLOS is influenced by climate variability, including seasonal variability, the El Niño–Southern Oscillation pattern and Pacific Decadal Oscillation (PDO) patterns.

The storm surge component was calculated by applying the wavelet filter on a 24–384-hour time window to the (detrended) tidal residual. Finally, the high-frequency variation left over from the tidal analysis was singled out by setting the filter to only pass signals with periods ranging from 6 hours to 12 hours.

Development of severe and extreme scenarios of wave and water level
through statistical analysis and numerical modelling
Bonriki, Tarawa, Kiribati

Extreme distribution analysis was performed for the total water level and the tidal residual. This approach consists of fitting the GPD to some high water level sample.

Thus, the analysis was performed using a POT method and by fitting a GDP to the peaks, defined as water level exceeding a defined threshold. The thresholds were selected based on the shape parameter of the distribution, the threshold stability property and the sensitivity of the 100-year return value. The 95% confidence interval was also calculated for each distribution. The EVA, threshold selection and confidence calculation were performed using the ORCA package (Deltares Systems 2012).

4.2. Results

4.2.1. Tide

Tidal constituents

Tide in Betio is semidiurnal and microtidal, with a form factor (Pugh 2004) of 0.17 and a tidal range of 1.80 m. The main tidal constituents are M2 (0.59 m), S2 (0.31 m) and N2 (0.12 m) (Table 2).

Table 2. *Harmonic constituents of the tidal signal at Betio.*

Constituent	M2	S2	N2	K1	K2	O1	P1	SA
Amplitude (m)	0.5898	0.3091	0.1237	0.0941	0.0862	0.0603	0.0304	0.0376
Phase (degrees)	139.44	152.76	137.48	68.61	147.54	41.87	66.56	273.49

The global tide is influenced by the 18.61-year lunar nodal cycle and the 8.85-year cycle of the lunar perigee. These cycles affect high tidal levels as an 18.6-year cycle and a 4.4-year cycle; the spring tides are higher than usual during the positive phase of the cycle, and lower than usual during the negative phase. The tidal record in Betio is too short to determine the amplitude of the 18.6-year cycle, but the range of the combined 4.4-year and 18.6-year cycles on the 99.9 percentile tidal levels is 0.02 m.

Exceedance curve

The mean high water perigean spring high tide, often referred to as the 'king tide', is the amplitude of the M2, S2 and N2 tidal harmonics. This tidal level (1.03 m) (Table 3) is exceeded by 8% of high tides. The mean high water spring tide is the combined amplitude of the M2 and S2 tidal harmonics (0.9 m); this is exceeded by 19% of high tides. The mean high water is the mean elevation of all high tides (0.65 m), and the mean high water neap is the difference in amplitude between the M2 and S2 tidal harmonics (0.28 m); this is exceeded by 90% of high tides (Figure 20).

Table 3. *Tide levels.*

	Mean high water perigean spring	Mean high water spring	Mean high water	Mean high water neap
Height above mean sea level (m)	1.03	0.9	0.65	0.28

Development of severe and extreme scenarios of wave and water level
through statistical analysis and numerical modelling
Bonriki, Tarawa, Kiribati
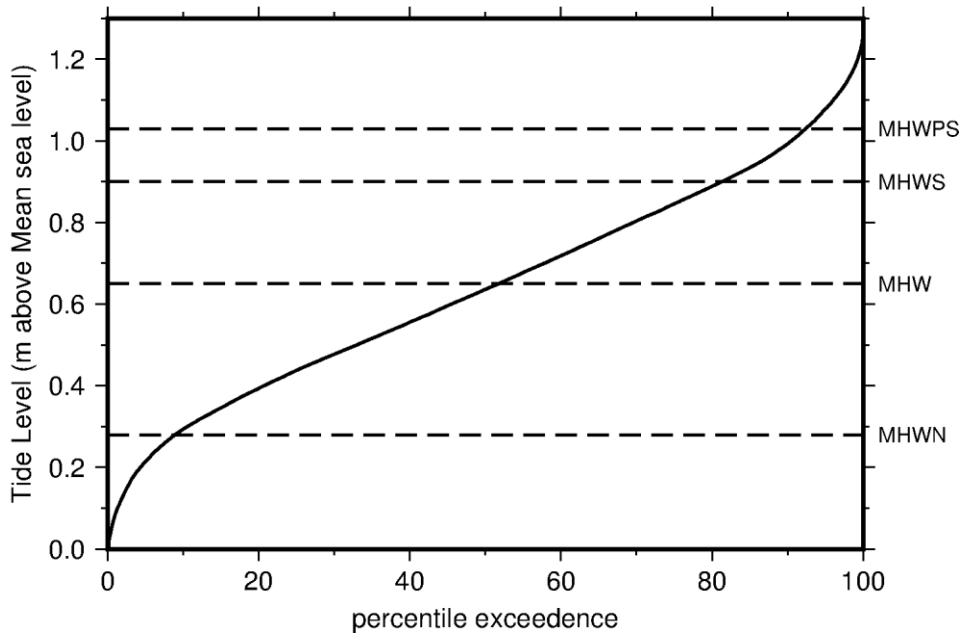
MHW = mean high water; MHWN = mean high water neap; MHWPS = mean high water perigean spring; MHWS = mean high water spring

Figure 20. *Tidal exceedance curve.*

4.2.2. Mean level of the sea and linear trend

Mean sea level variations are influenced by weather patterns across the Pacific Ocean, such as the strength and orientation of trade winds, sea surface temperature and the depth of the thermocline – all of these can be influenced by El Niño/La Niña events.

As well as being influenced by tides, the water level at Betio is influenced by long-term sea level anomalies and storm surges. The MLOS shows the long-term anomalies. We detrended the MLOS and found a linear trend of 3.8 mm/year over the past 21.4 years, from 1993 to 2014 (Figure 21). This linear increase in water level recorded at the tide gauge cannot be attributed to climate change alone, since changes in atmospheric pressure and vertical ground movement are potentially significant contributors. As well, a 21-year period is not sufficient to provide confidence in a trend of sea level rise.

Sea level reconstruction over the period 1950–2009 identified a 2.7 mm/year increase in the MLOS at Tarawa (Becker et al. 2012).

The largest variation in the record occurred during the 1997–98 El Niño event, with the MLOS reaching 0.245 m above the mean sea level trend on 17 March, 1997, and 0.250 m below the mean sea level trend on 14 February, 1998. During that El Niño/La Nina event, the changes in MLOS corresponded with 20% of the tidal range.

Development of severe and extreme scenarios of wave and water level
through statistical analysis and numerical modelling
Bonriki, Tarawa, Kiribati
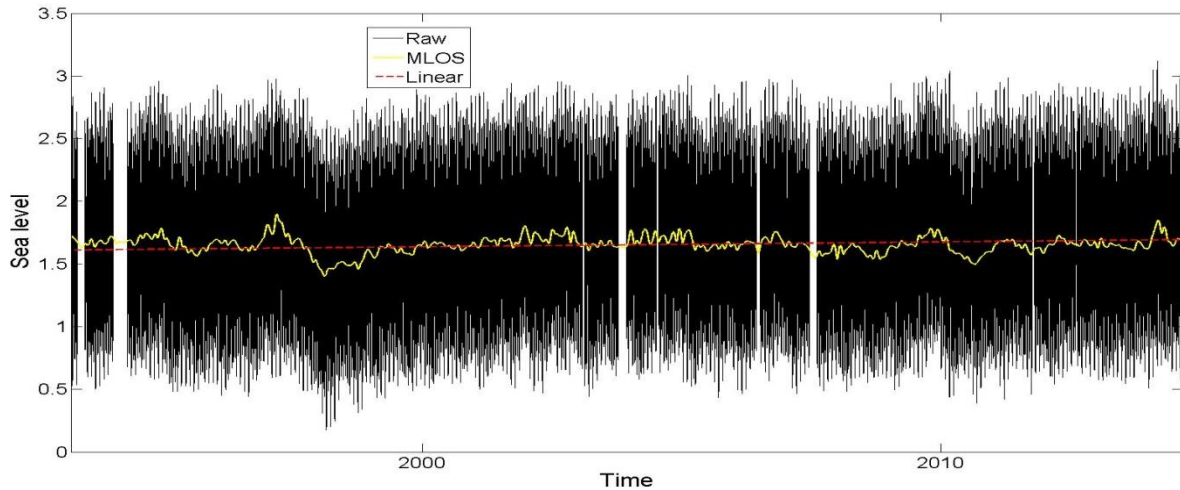
MLOS = mean level of the sea

Figure 21. Plot overlaying 21.4 years of tide gauge records, mean level of the sea and linear trend

The monthly MLOS is very variable, at 0.042 m – this is 4% of the typical tidal range over the past 20 years. However, climate variability phenomena such as El Niño can disrupt the consistency of this signal. Again, the El Niño event of 1997–98, with the highest and lowest monthly MLOS recorded at the Betio tide gauge, in February 1997 and March 1998, respectively, is seen in Figure 22.
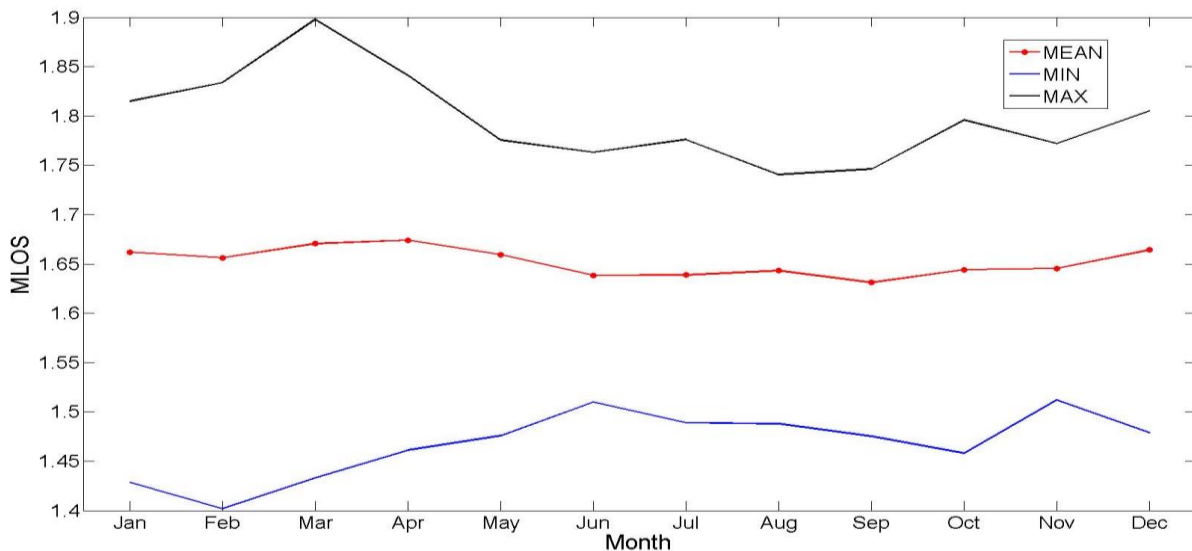
Figure 22. *Monthly variation of mean level of the sea (MLOS).*

4.2.3.   Storm surge

Storm surges in Betio have exceeded 0.10 m on three occasions since 1993. The typical range (i.e. standard deviation) of the storm surge is 0.02 m. The storm surge calculated at Betio is not expected to reach above 0.13 m for an event with a return interval of 100 years

The storm surge is expected to be small in the region because of the lack of continental shelf surrounding the Tarawa atoll. Most of the storm surge can probably be attributed to wind set-up, but further analysis would be required to verify this hypothesis. Although storm surge is a major

Development of severe and extreme scenarios of wave and water level
through statistical analysis and numerical modelling
Bonriki, Tarawa, Kiribati

contributor to coastal flooding near continental masses or in areas prone to tropical cyclones, it is not the main contributor to coastal flooding in Tarawa.
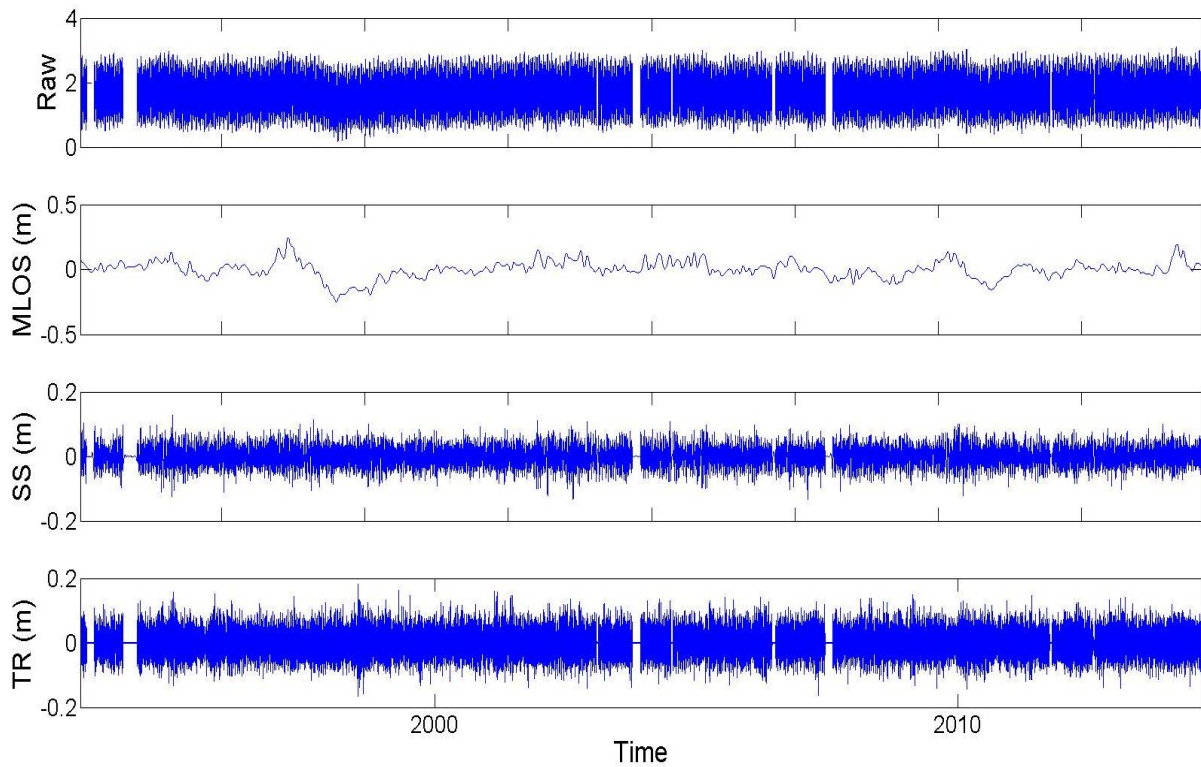
MLOS = mean level of the sea; SS = storm surge; TR = remaining high-frequency signal

Note: The top figure shows the raw signal recorded at the tide gauge.

Figure 23. Decomposition of the tidal residual into mean level of the sea, storm surge and high-frequency signal.

Development of severe and extreme scenarios of wave and water level
through statistical analysis and numerical modelling
Bonriki, Tarawa, Kiribati
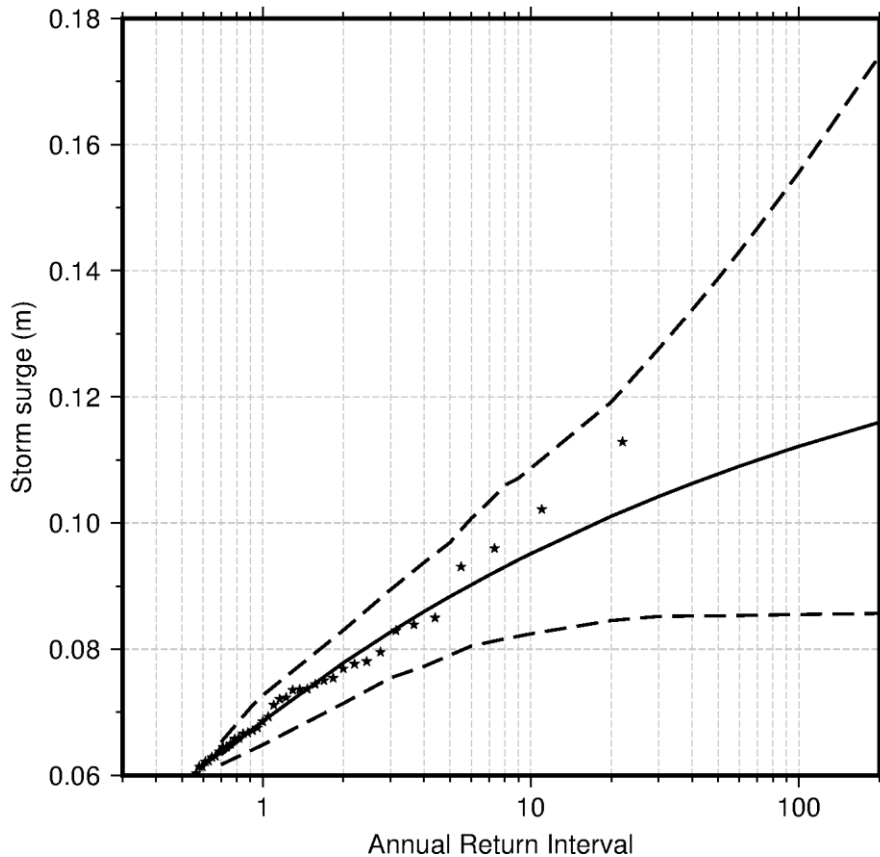
Note: Data are shown by stars. The solid line shows the best fit to the extreme values; the dashed lines show the 95% confidence limits of the fit.

Figure 24. *Extreme value distribution of storm surge.*

4.2.4. Extreme distribution

Extreme value analysis on the total water level

The tide gauge data are further processed to estimate the frequency and magnitude of high storm tide levels. Storm tide includes the effect of tide, storm surge and MLOS.

Since the inundation model (BIVA inundation modelling report) uses Hawaii Tide Gauge Zero (HTGZ) as its vertical reference datum, the water levels have been reduced to HTGZ. A shift between the SEAFRAME and HTGZ data of 0.419 m, as found by Ramsey et al. (2008), was applied before EVA was undertaken.

Extreme distribution of water level can be assessed directly from the total water level, as measured by the tide gauge (Figure 25).

Development of severe and extreme scenarios of wave and water level
through statistical analysis and numerical modelling
Bonriki, Tarawa, Kiribati

Note: The solid line shows the best fit to the extreme values; the dashed lines show the 95% confidence limits of the fit.

Figure 25. *Extreme value distribution on tide gauge data recorded at Betio, Tarawa.*

The GDP fitted to the peaks above a selected threshold (Figure 26) has a 100-year return interval value of 2.63 m above the HTGZ reference datum. The high water levels selected by the POT over the raw tide gauge data are highly dependent on the co-occurrence of spring high tide and high tidal residual over the past 21.4 years.

Convolution between astronomical tide and tidal residual

Another approach can also be used, based on the assumption that tidal signal and tidal residual are independent at the Betio tide gauge. The extreme values of still water level can then be estimated by the convolution of the extreme distribution of the tidal residual and the empirical distribution of the tidal level. This approach takes advantage of the information on the astronomical tide gained by processing the 21 years of tidal record.

High tidal residual values picked from the POT (Figure 27) were fitted to the GDP. After convolution with the tide (Figure 29), the 100-year return value of still water level is 2.74 m above HTGZ – 11 cm higher than the value obtained when performing the EVA on the raw data.

The convolution between tide and tidal residual did not generate superior results when used on a long tidal record of about 120 years (Caires et al. 2007). However, on the limited still water level

Development of severe and extreme scenarios of wave and water level
through statistical analysis and numerical modelling
Bonriki, Tarawa, Kiribati

record at the Betio tide gauge, the co-occurrences of the meteorological and the astronomical effects captured in the past 21 years appear to significantly affect the outcome of the EVA.
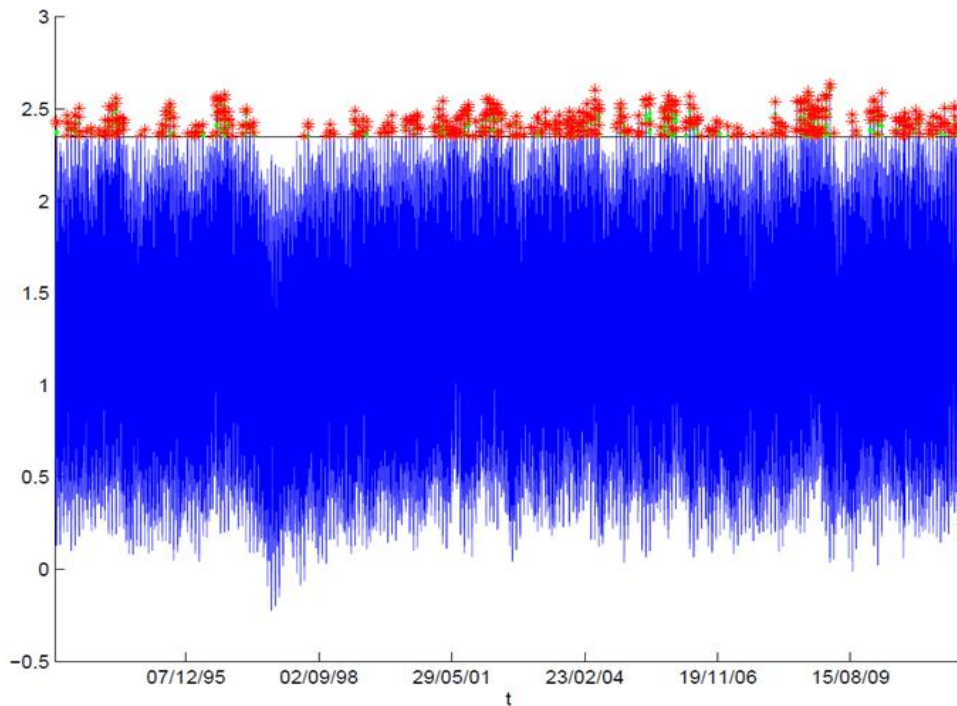
Figure 26. *Peaks-over-threshold analysis on raw water level.*
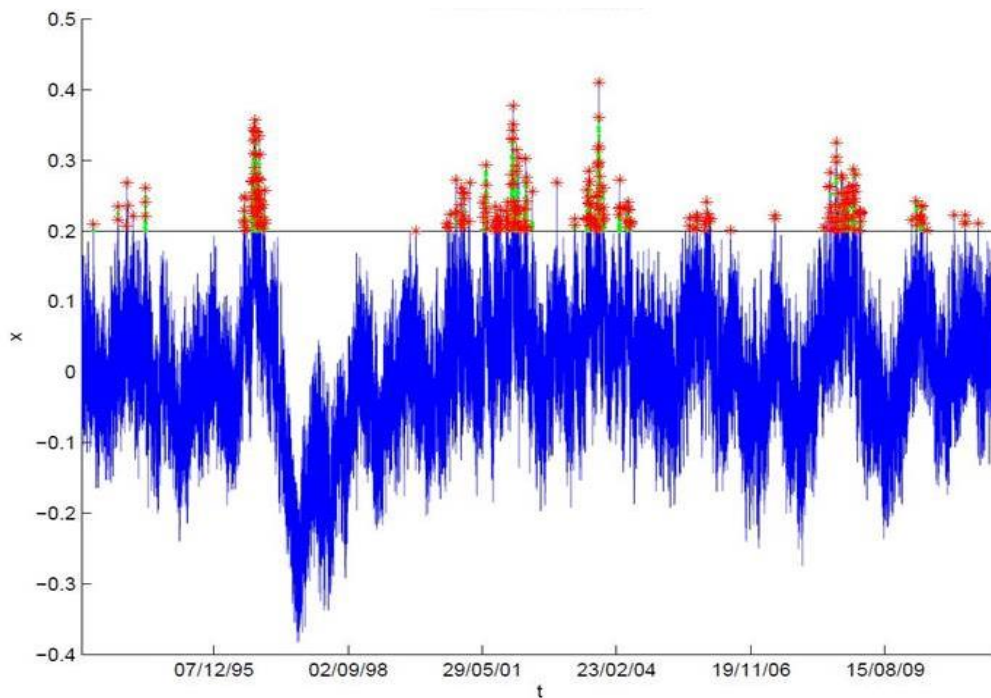
Figure 27. *Peaks-over-threshold analysis on tidal residual (difference between raw tide gauge data and predicted tide).*

Development of severe and extreme scenarios of wave and water level
through statistical analysis and numerical modelling
Bonriki, Tarawa, Kiribati
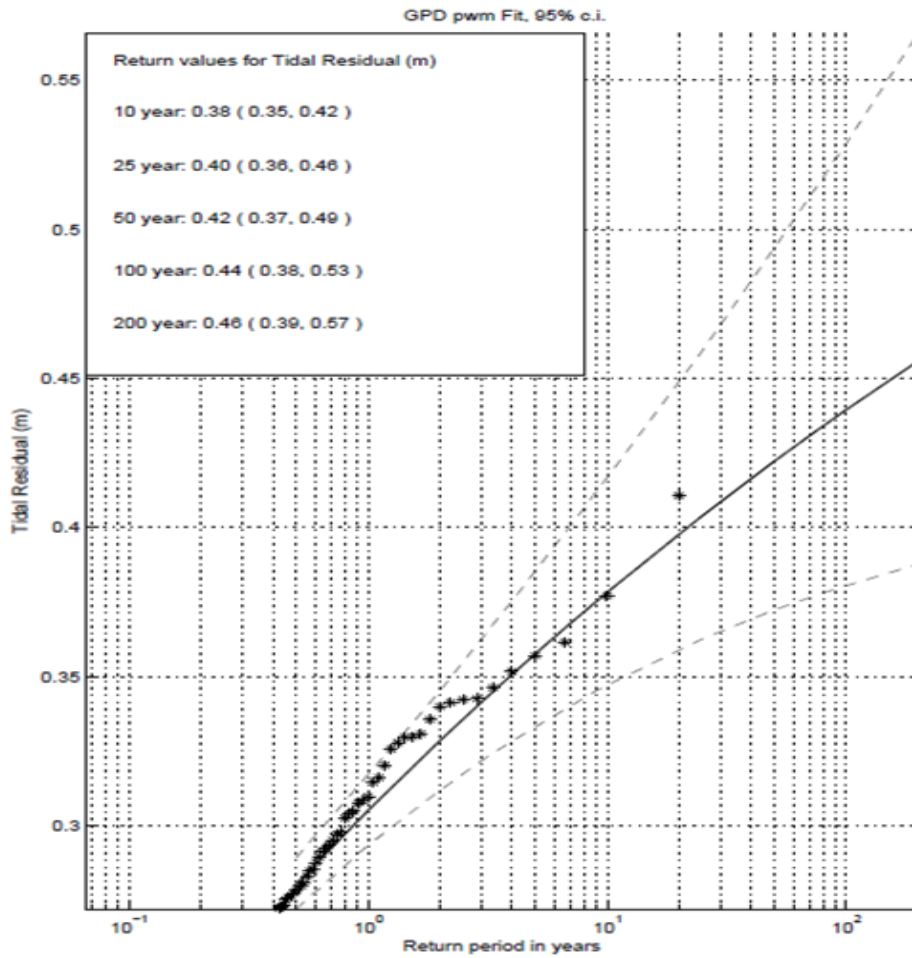
Note: The plain line shows the best fit to the extreme values; the dashed lines show the 95% confidence limits of the fit.
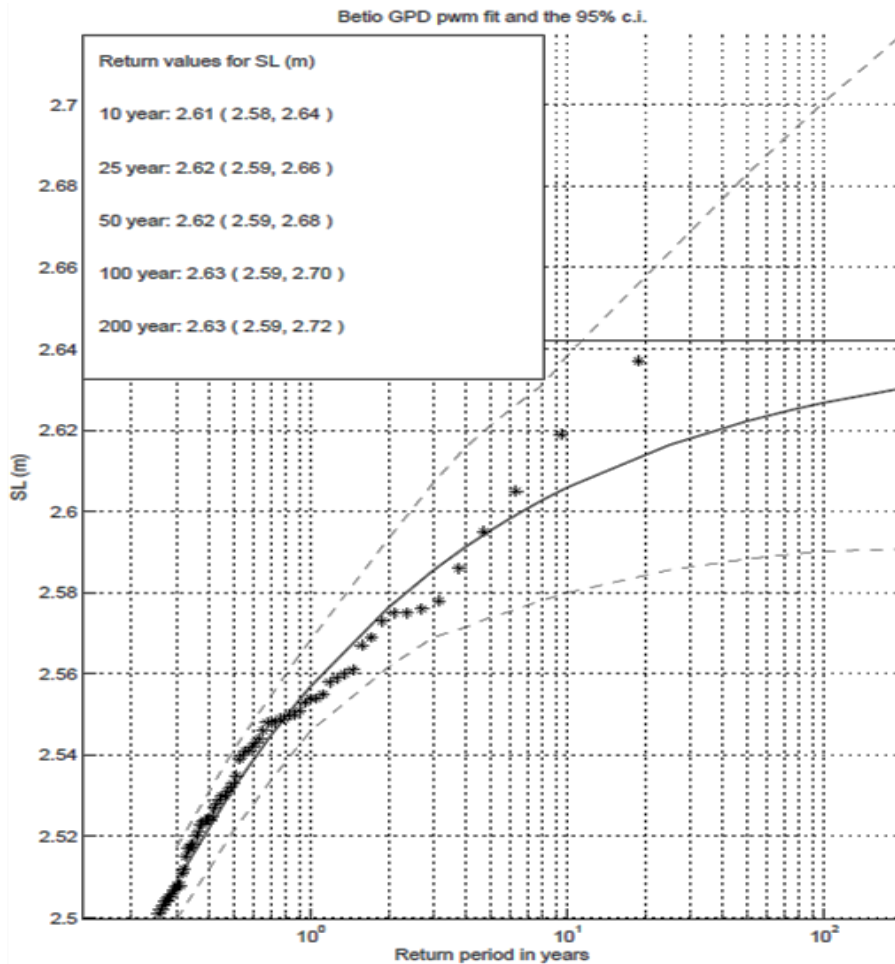
Figure 28. *Extreme value distribution on the tidal residual derived from tide gauge data recorded at Betio, Tarawa.*

Development of severe and extreme scenarios of wave and water level
through statistical analysis and numerical modelling
Bonriki, Tarawa, Kiribati
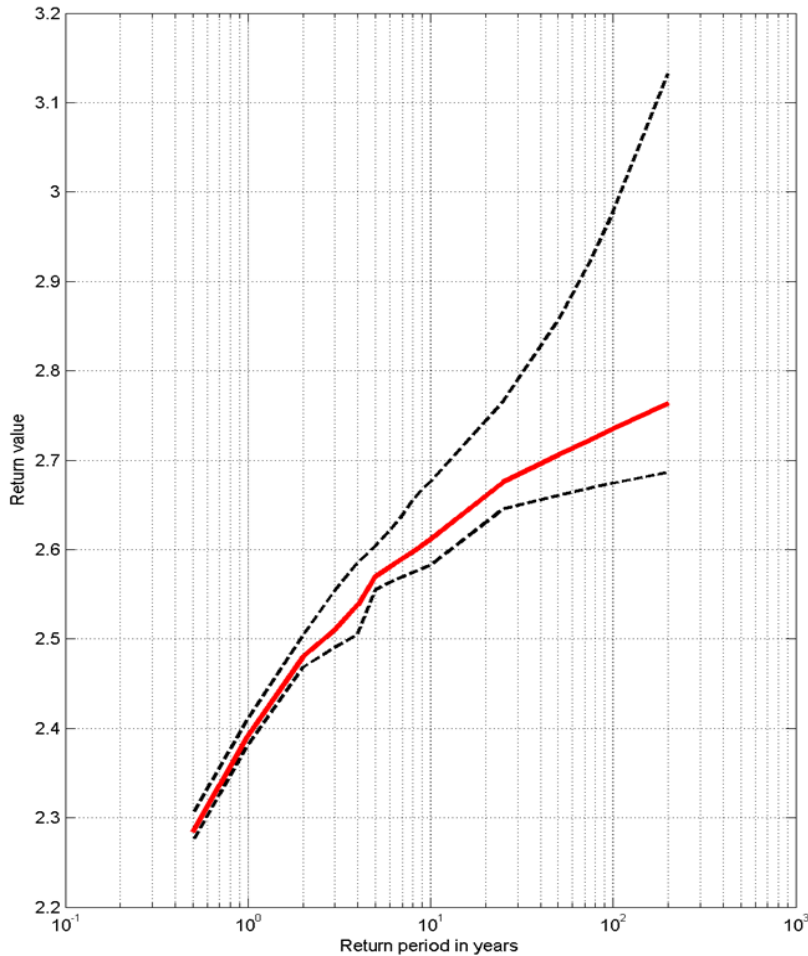
Figure 29. *Convolution between extreme value of tidal residual and empirical tidal levels at Betio.*

4.3. Discussion

Based on the total water level, this study found a storm tide for a 100-year return interval that is consistent with previous calculations from Ramsay et al. (2008). This is to be expected, because the current study used a similar methodology and 50% of the same data used by Ramsay et al. (2008).

However, this result is highly dependent on the co-occurrence of the peaks from each component of the tide gauge record: MLOS, storm surge and the astronomical tide.

This study also investigated the convolution between astronomical tide and the extreme distribution of the tidal residual. This result in a storm tide of 2.74 m for a 100-year return interval, which is 11 cm higher than the tide based on the total water level.

This convolution results in an extreme distribution of storm tide that is independent of the co-occurrence of the astronomical tide and tidal residual recorded at the tide gauge over the last 21 years.

Although this methodology represents a step forward in estimating the extreme storm tide distribution at the Betio tide gauge, the result is still potentially influenced by the recorded co-occurrence of the storm surge and the MLOS.

Development of severe and extreme scenarios of wave and water level
through statistical analysis and numerical modelling
Bonriki, Tarawa, Kiribati

The storm tide level at Betio was applied offshore at Bonriki. MLOS, astronomical tide and barometric pressure components of the storm surge are assumed to be identical in the ocean and at the Betio tide gauge. However, the wind set-up is expected to be higher at the Betio tide gauge than on the ocean shoreline. Wind set-up on the ocean shoreline is estimated following an empirical relation, based on the momentum balance of the wind stress and the water surface gradient:

$$\Delta \eta_{wind} = \frac{W C_d U^2}{K(h_r + \Delta \eta_{wave})}$$

where

W is the width of the reef flat

C_d is the wind drag coefficient (approximated following Smith [1980]: $C_D = 0.44 + 0.063\ U_{10}$)

U is the wind speed

K is an empirical coefficient (in the range of 800,000–1,200,000; Sánchez et al. 2007)

h_r is the still-water depth over the reef flat

$\Delta \eta_{wave}$ is the wave set-up.

Wind data recorded by the meteorological station at Betio (under the Climate and Oceans Support Program in the Pacific) are used to compute the wind set-up at the Bonriki ocean shoreline by considering only easterly winds (20–160°). The estimated wind set-up at the ocean shoreline of Bonriki peaks at 0.2 mm. Therefore, applying the storm tide level from the Betio tide gauge on the ocean side of Bonriki is considered an appropriate conservative approach.

As part of the Kiribati Adaptation Programme (Ramsay et al. 2008), the hydrodynamic model of Tarawa developed by SOPAC (Damlamian and Kruger, 2008) was used to assess wind set-up along the lagoon coastline of Tarawa.

Results show a variability of storm tide in the lagoon of 0.03 m (Ramsay et al. 2008). The extreme distribution of storm tide at Betio is only 1 cm lower than on the southeast corner of the lagoon, near Bonriki. Ramsay et al. (2008) also found that this result applies under a sea level rise of 0.48 m, and suggests that higher water levels near Bonriki are caused by tidal amplification and wind set-up during westerly winds.

Development of severe and extreme scenarios of wave and water level
through statistical analysis and numerical modelling
Bonriki, Tarawa, Kiribati

5. Climate Change Projection

The fourth assessment report (AR4) of the Intergovernmental Panel on Climate Change (IPCC) used three scenarios of climate change, based on differences in the factors driving greenhouse gas emissions, such as population growth.

The most recent IPCC report, AR5, used a different approach to develop four scenarios. The scenarios, or representative concentration pathways (RCPs), are based on possible increases in the energy the earth will retain by 2100, as a result of human activity. This is used to derive the concentration of greenhouse gases needed to trap that energy, and its effect on climate.

The four RCPs are as follows.

- RCP2.6 is an aggressive mitigation pathway.
- RCP4.5 describes greenhouse gas concentrations stabilising at about 540 ppm by 2100.
- RCP6.0 describes greenhouse gas concentrations reaching about 670 ppm by 2100 and stabilising at around 750 ppm thereafter.
- RCP8.5 describes a continued warming. Greenhouse gas concentrations reach about 940 ppm by 2100 and stabilise at approximately 2,000 ppm (seven times higher than preindustrial levels) by 2250.

AR5 predicts that global sea level will rise more than previously projected by 2100. The report predicts a global sea level rise by 2100 of between 0.29 m and 0.82 m, under all four RCPs. The increased prediction for sea level rise between AR4 and AR5 is mainly the result of improved observation and physical understanding of changes in ice sheet dynamics.

Under the PACCSAP project, the Commonwealth Scientific and Industrial Research Organisation (CSIRO) and the Australian Bureau of Meteorology investigated the projection from the four new RCPs for each Pacific country, using a global climate model based on the Coupled Model Intercomparison Project Phase 5 (CMIP5).

Results for the Gilbert Group, where Tarawa is located, show a sea level rise of 23–87 cm by 2090.

Although the use of process-based models is considered to be the most scientifically sound approach, much uncertainty remains in projections from these models. There is only a medium confidence (66% certainty) in AR5 predictions for sea level rise; this is a significant improvement from AR4, which gave no indication of likelihood. The IPCC estimates the risk of exceeding its upper limit to be about 17%. The uncertainty in sea level rise prediction is largely due to the lack of current understanding about possible collapse of large ice sheets in Antarctica and Greenland. The latest IPCC report mentions that, if marine-based ice-sheets in Antarctica collapse, sea level rise could increase by several tenths of a metre.

Since the IPCC does not provide upper limits to its projections, NOAA (Parris et al. 2012) developed scenarios (using combined semi-empirical and process-based models) specifically for the purpose of coastal planning, policy and management. From their scenarios, sea level rise projections by 2100 range from 0.2 m to 2 m, with a very high confidence (90%) in the outcome. Their approach is

Development of severe and extreme scenarios of wave and water level
through statistical analysis and numerical modelling
Bonriki, Tarawa, Kiribati

consistent with guidance from the US Army Corps of Engineers for coastal decision makers who are assessing coastal impacts and vulnerabilities.

NOAA provides four scenarios to help assess the key uncertainties – the rate and magnitude of ocean warming and ice sheet loss – surrounding estimates of future global sea level rise.
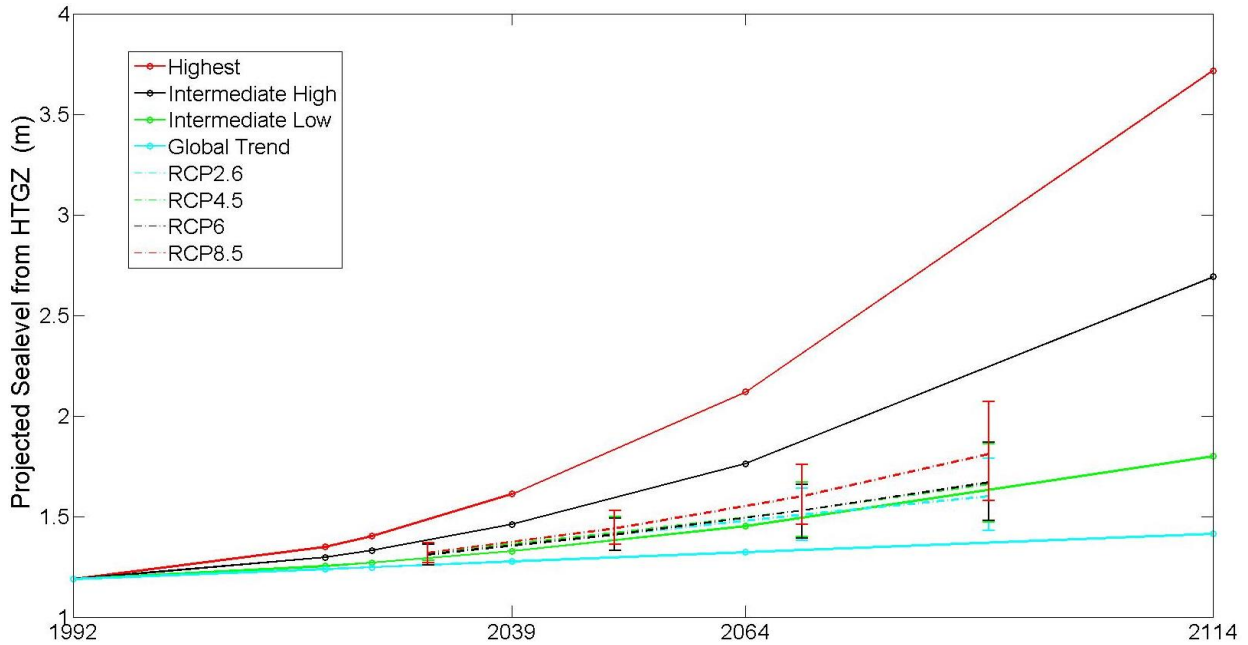
- The **highest** scenario is derived from a combination of estimated ocean warming from the IPCC AR4 global sea level rise projections and a calculation of the maximum possible glacier and ice sheet loss by the end of the century. This scenario should be considered in situations where there is little tolerance for risk (e.g. new infrastructure with a long anticipated life cycle, such as a power plant).

- The **intermediate–high** scenario is based on an average of the high end of semi-empirical, global sea level rise projections. Semi-empirical projections use statistical relationships between observed global sea level change, including recent ice sheet loss, and air temperature. The intermediate–high scenario allows experts and decision makers to assess risk from limited ice sheet loss.

- The **intermediate–low** scenario is based on the upper end of the AR4 global sea level rise projections resulting from climate models using the B1 emissions scenario. This scenario allows experts and decision makers to assess risk primarily from ocean warming.

- The **lowest** scenario is based on a linear extrapolation of the historical rate of sea level rise derived from tide gauge records beginning in 1900 (1.7 mm/year). Since the 1990s, the rate of sea level rise has increased to 3.2–3.6 mm/year. However, the length of the record (~20 years) does not allow any extrapolation into the next century.

The sea level rise projections based on the RCPs are between NOAA's intermediate–low and intermediate–high scenarios (Figure 30). This is because semi-empirical models of ice sheet loss (i.e. based on and calibrated against past events) give higher projections of sea level rise than process-based models.

Although IPCC projections describe the most likely future we can currently predict, they do not encompass the full range of possible sea level rise projections.

To keep the number of scenarios manageable, three climate change scenarios were chosen: RCP6 and RCP8.5 from the IPCC, and the intermediate–high scenario from NOAA (as a more conservative approach). The intermediate-high scenario from NOAA is more in line with the recommendation by Anders Levermann (one of the co-authors of the IPCC chapter on sea level rise) for an upper limit for sea level rise by 2100 of about 1.5 m for practical coastal management work.[1]

---

[1] http://e360.yale.edu/feature/yale_e360_forum_on_ipcc_report_2013/2698

Development of severe and extreme scenarios of wave and water level
through statistical analysis and numerical modelling
Bonriki, Tarawa, Kiribati

HTGZ = Hawaii Tide Gauge Zero

Figure 30. *Projected sea level rise in Tarawa using the IPCC and NOAA scenarios.*

In this study, a 50-year (to 2064) sea level rise projection was selected to build the scenarios. The projections are 0.22 m, 0.28 m and 0.49 m for the RCP6, RCP8.5 and intermediate–high scenarios, respectively.

Ramsay et al. (2008) investigated the impact of sea level rise on the extreme wave height in the lagoon. Near Bonriki, the study showed an increase of about 6 cm for the 10-year, 50-year and 100-year return interval significant wave heights, for a sea level rise projection of 0.48 m. The intermediate–high scenario used as an upper limit in the current study shows a sea level rise of 0.49 m for 2064. Thus, the impact of sea level rise on wave height at Bonriki ranges from 0 cm to 6 cm for all scenarios.

The projected wave climate for the Gilbert Islands was investigated under the PACCSAP project by the Australian Bureau of Meteorology and CSIRO based on the four scenarios in AR5. Wave height is projected to decrease between December and March, with a decrease of about 20 cm in storm wave. However, wave climate projection is at an early stage, and uncertainty in the predictions is high.

In this study, the 10-year, 50-year and 100-year return interval wave heights are fixed for all climate change scenarios. This decision was taken by considering the following.

- The impact of sea level rise on the wave height at Bonriki (lagoon side) is small (0–6 cm); sea level rise is therefore assumed to have no significant impact on potential inundation. As well, the potential change of wave height is well within the 95% confidence zone of the 10-year and 50-year return interval; it is small compared with the 95% confidence zone of the 100-year return interval.

- Although wave height is projected to decrease in the Gilbert Islands, there is a low confidence in this projection.

Development of severe and extreme scenarios of wave and water level
through statistical analysis and numerical modelling
Bonriki, Tarawa, Kiribati

6. Joint Probability of Exceedance

The EVA estimates the annual return interval for high storm tide and high wave height; however, inundation events are often triggered by the co-occurrence of the two processes. As discussed in Ramsay et al. (2008), there is only a low correlation between storm tide and large waves in Tarawa.

To determine the likelihood of an event characterised by co-occurrence of a high storm tide and a large wave, both datasets were combined to perform a joint probability analysis for both sides of Bonriki: in the lagoon and on the reef slope (at ~18 m depth). This process used the JOIN-SEA software developed by HR Wallingford and Lancaster University.

Joint probability analysis requires simultaneous values of storm tide and wave height. Thus, the 34-year hindcast wave data were cropped to fit the 21 years of tide gauge records available at the time of this analysis (1993–2013).The outcome of the EVA performed on wave height and storm tide was incorporated back into the calculation before generating a long-term time series. The final joint probability of high storm tide and large waves are derived from this generic long-term time series (Figures 31 and 32).
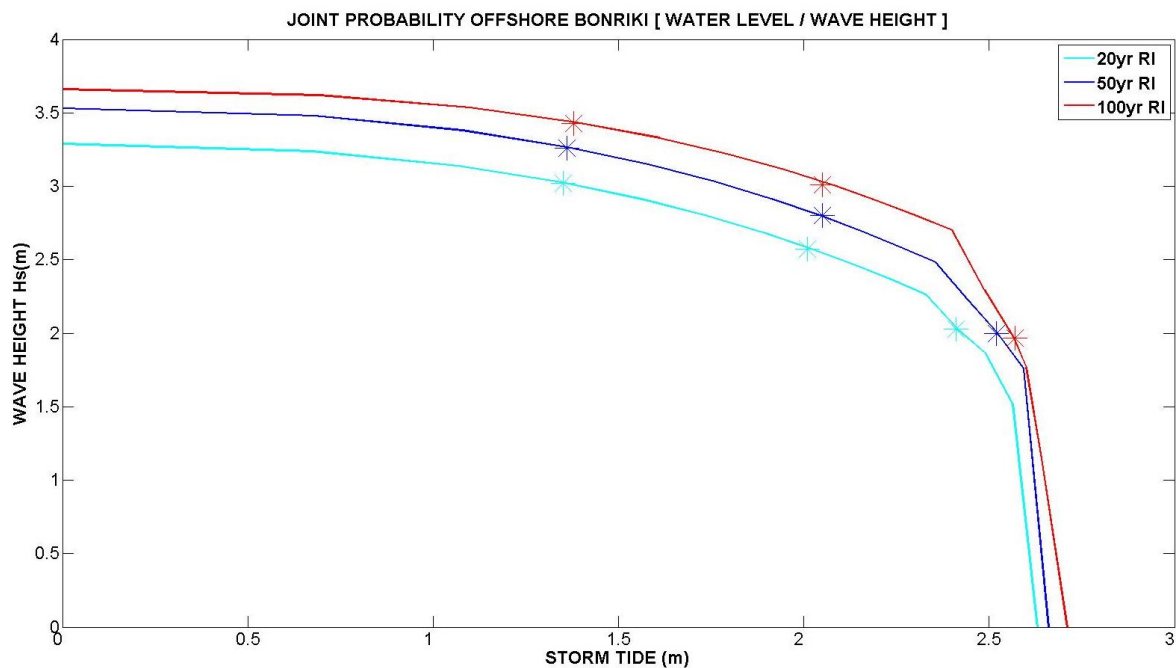
AEP = annual exceedance probability

Figure 31. *Joint probability between storm tide and wave height on the reef slope (~18 m depth) off Bonrik. The figure shows the 5% AEP (light blue line), 2% AEP (dark blue line) and 1% AEP (red line). See Figure 33 for more details on the relationship between return intervals and annual exceedance probabilities.*

Development of severe and extreme scenarios of wave and water level
through statistical analysis and numerical modelling
Bonriki, Tarawa, Kiribati

AEP = annual exceedance probability

Figure 32. *Joint probability between storm tide and wave height in the lagoon (~5 m depth) near Bonriki. The figure shows the 5% AEP (light blue line), 2% AEP (dark blue line) and 1% AEP (red line). See Figure 33 for more details on the relationship between return intervals and annual exceedance probabilities.*

AEP = annual exceedance probability; ARI = annual return interval

Note: P (probability of occurrence within planning lifetime) = 1-e^ (-L)/ARI

Source: adapted from King, 2010

Figure 33. *Likelihood of an event with a specified probability of occurrence (AEP or ARI) occurring within planning lifetimes. For example, a 100 year return interval event, which has a 1% chance of occurring in any one year, has a propability of 63% to occur over the planning lifetime of 100 years.*

Development of severe and extreme scenarios of wave and water level
through statistical analysis and numerical modelling
Bonriki, Tarawa, Kiribati

7. Scenarios

The outcome of the joint probability analysis and computation of projected sea level rise were used to define the scenarios to be fed into the inundation model (BIVA inundation modelling report). Seventy-two scenarios were established to investigate the probabilistic inundation hazard of Bonriki Islet.

Based on the joint probability analysis, three scenarios were chosen for each of the 20-year return interval, 50-year return interval and 100-year return interval lines (as shown by the stars in Figures 31 and 32). This generates nine scenarios under the current sea level on each side of Bonriki.

These scenarios were also investigated under the three climate change scenarios described under 'Climate Change Projection': RCP6, RCP8.5 and NOAA's intermediate–high scenario. For this, sea level rise projections for 2064 (50 years from now) were added to the storm tide of each scenario.

Because of the low confidence in the projected change in waves due to climate change, and the small change (weighed against the high computation time needed to run a high-resolution SWAN model over Tarawa), the wave height remains fixed for all climate change scenarios.

However, in the lagoon, a rise of about 50 cm (the maximum sea level rise investigated in this study) could potentially lead to a significant change in wave height near Bonriki. However, Ramsay et al. (2008) found that, under a sea level rise of 50 cm, wave height near Bonriki would only increase Hs by 5 cm. The change in wave height associated with sea level rise is thought to be negligible, especially when compared with the EVA 95% confidence zone.

Table 4. *Offshore scenarios.*

	ID	NO SLR Scenario		ID	SC1 +22cm		ID	SC2 +28cm		ID	SC3 +49cm	
OFFSHORE												
		WL	Hs		WL	Hs		WL	Hs		WL	Hs
20 yrs	1	1.35	3.02	4	1.57	3.02	7	1.63	3.02	10	1.84	3.02
	2	2.01	2.57	5	2.23	2.57	8	2.29	2.57	11	2.5	2.57
	3	2.41	2.03	6	2.63	2.03	9	2.69	2.03	12	2.9	2.03
50 yrs	13	1.36	3.26	16	1.58	3.26	19	1.64	3.26	22	1.85	3.26
	14	2.05	2.8	17	2.27	2.8	20	2.33	2.8	23	2.54	2.8
	15	2.52	2	18	2.74	2	21	2.8	2	24	3.01	2
100 yrs	25	1.38	3.43	28	1.6	3.43	31	1.66	3.43	34	1.87	3.43
	26	2.08	3	29	2.3	3	32	2.36	3	35	2.57	3
	27	2.56	1.969	30	2.78	1.969	33	2.84	1.969	36	3.05	1.969

Hs = significant wave height; SC = climate change scenario; WL = water level or storm tide

Development of severe and extreme scenarios of wave and water level
through statistical analysis and numerical modelling
Bonriki, Tarawa, Kiribati

Table 5. *Lagoon scenarios.*

	ID	NO SLR Scenario		ID	SC1 +22cm		ID	SC2 +28cm		ID	SC3 +49cm	
		WL	Hs		WL	Hs		WL	Hs		WL	Hs
20 yrs	1	2	0.84	4	2.22	0.84	7	2.28	0.84	10	2.49	0.84
	2	2.44	0.65	5	2.66	0.65	8	2.72	0.65	11	2.93	0.65
	3	2.66	0	6	2.88	0	9	2.94	0	12	3.15	0
50 yrs	13	2.08	0.93	16	2.3	0.93	19	2.36	0.93	22	2.57	0.93
	14	2.48	0.716	17	2.7	0.716	20	2.76	0.716	23	2.97	0.716
	15	2.71	0	18	2.93	0	21	2.99	0	24	3.2	0
100 yrs	25	2.11	0.99	28	2.33	0.99	31	2.39	0.99	34	2.6	0.99
	26	2.52	0.766	29	2.74	0.766	32	2.8	0.766	35	3.01	0.766
	27	2.75	0	30	2.97	0	33	3.03	0	36	3.24	0

Hs = significant wave height (m); SC = climate change scenario; WL = water level or storm tide (m)

Development of severe and extreme scenarios of wave and water level
through statistical analysis and numerical modelling
Bonriki, Tarawa, Kiribati

8. Conclusion

Coastal inundation is a constant concern on low-lying islands such as the Tarawa atoll, Kiribati. Because Tarawa is close to the equator (latitude 1°N), it is not threatened by cyclone-generated inundation. Rather, inundation is expected to be triggered by high storm tide levels or swells, or the co-occurrence of the two processes. Inundation generated from tsunamis is not considered in this study.

In this study, the occurrence of extreme wave height and extreme storm tide at Bonriki (on Tarawa atoll) is examined, based on numerical modelling (SWAN) and the tide gauge record, respectively. The possible joint occurrence of high storm tide and high waves is then investigated through a joint probability analysis. Finally, three climate change projections are used to examine the potential exacerbation of inundation risk from sea level rise.

This study proposes a total of 72 probabilistic scenarios characterised by wave height, storm tide and climate change scenarios. The potential inundation generated from these scenarios is investigated numerically in a companion report (BIVA inundation modelling report).

Development of severe and extreme scenarios of wave and water level
through statistical analysis and numerical modelling
Bonriki, Tarawa, Kiribati

9. References

Becker, M., Meyssignac, B., Letetrel, C., Llovel, W., Cazenave, A. and Delcroix, T. 2012. Sea level variations at tropical Pacific islands since 1950. Global and Planetary Change 80–81:85–98. doi:10.1016/j.gloplacha.2011.09.004.

Brier, G.W. 1950. Verification of forecasts expressed in terms of probability. Monthly Weather Review 1–3.

BoM (Australian Bureau of Meteorology) 2010. Pacific country report, sea level and climate, Kiribati. South Pacific Sea Level and Climate Monitoring Project.

Caires, S., Diermanse, F., Dillingh, D. and de Graaff, 2007, R. Extreme still water levels. Proc. of the 10th int. workshop on wave hindcasting and forecasting and Coastal Hazard Symposium,WMO/TD-No. 1442, Hawaii, U.S.A, 11-16 November 2007.

Church, J.A., White, N.J. and Hunter, J.R. 2006. Sea-level rise at tropical Pacific and Indian Ocean islands. Global and Planetary Change 53(3):155–168. doi:10.1016/j.gloplacha.2006.04.001.

Coles, S. 2001. An introduction to statistical modeling of extreme values. London: Springer-Verlag.

Deltares Systems 2012. ORCA, analysis, classification and transformation of metocean data. User manual.

Durrant, T., Greenslade, D., Hemer, M. and Trenham, C. 2014. A global wave hindcast focussed on the central and south Pacific. CAWCR Technical Report 070. Australia: Centre for Australian Weather and Climate Research.

King, J. 2010. A guide for local government in New Zealand. Ministry for the Environment. ME 1012.

KNSO and SPC 2012. Kiribati 2010 census. Volume 2, Analytical report. Kiribati National Statistics Office and the Secretariat of the Pacific Community Statistics for Development Program

Komen, G.J., Hasselmann, S. and Hasselmann, K. 1984. On the existence of a fully developed wind–sea spectrum. Journal of Phyical Oceanography 14:1271–1285.

Madsen, O.S., Poon, Y.-K. and Graber, H.C. 1988. Spectral wave attenuation by bottom friction: theory. p. 492–504. In: Proceeding of the 21st International Conference on Coastal Engineering. New York: American Society of Civil Engineering.

Merrifield, M.A., Thompson, P.R. and Lander, M. 2012. Multidecadal sea level anomalies and trends in the western tropical Pacific. Geophysical Research Letters 39(13). doi:10.1029/2012GL052032.

Meyssignac, B., Salas y Melia, D., Becker, M., Llovel, W. and Cazenave, A. 2012. Tropical Pacific spatial trend patterns in observed sea level: internal variability and/or anthropogenic signature? Climate of the Past 8(2):787–802. doi:10.5194/cp-8-787-2012.

Pawlowicz, R., Beardsley, B. and Lentz, S. 2002. Classical tidal harmonic analysis including error estimates in MATLAB using T_TIDE. Computers and Geosciences 28:929–937.

Development of severe and extreme scenarios of wave and water level
through statistical analysis and numerical modelling
Bonriki, Tarawa, Kiribati

Pugh, D.T. 2004. Changing sea levels: effects of tides, weather and climate. Cambridge, UK: Cambridge University Press.

Ramsay, D., Stephens, S., Gorman, R., Oldman, J. and Bell, R. 2008. Kiribati Adaptation Programme. Phase II: Information for climate risk management. Sea level, waves, run-up and overtopping. Report prepared for the Government of Kiribati by the National Institute of Water and Atmospheric Research (New Zealand).Saha, S., Moorthi, S., Pan, H., Wu, X., Wang, J., Nadiga, S. et al. 2010. The NCEP climate forecast system reanalysis. Bulletin of the American Meteorological Society 91(8):1015–1057.

Sánchez, A., McKee Smith, J., Demirbilek, Z. and Boc, S. 2007. Combined wind and wave over a fringing reef. Vicksburg, Mississippi: Coastal Hydraulics Laboratory, US Army Corps of Engineers.

Smith, S. 1980. Wind stress and heat flux over the ocean in gale force winds. Journal of Physical Oceanography 10:709–726.Tolman, H. 1991. A third-generation model for wind waves on slowly varying, unsteady, and inhomogeneous depths and currents. Journal of Physical Oceanography 21(6):782–797.

Tolman, H. 2009. User manual and system documentation of WaveWatch III TM version 3.14. Camp Springs, Maryland: United States Department of Commerce, National Oceanic and Atmospheric Administration, National Weather Service, National Centers for Environmental Prediction.

Damlamian and Kruger, 2008, Hydrodynamic Model of Tarawa. Water Circulation and Applications. SOPAC Project Report 134Parris et al, 2012. Global sea level rise scenarios for United States national climate assessment, NOAA technical Report OAR CPO-1.

CONTACT DETAILS
Secretariat of the Pacific Community